Review

Chinese Science Bulletin

SPECIAL TOPIC
Carbon Nanotubes

January 2012 Vol.57 No.2-3: 205–224
doi: 10.1007/s11434-011-4878-0

Freestanding single-walled carbon nanotube bundle networks: Fabrication, properties and composites

ZHOU WeiYa*, MA WenJun, NIU ZhiQiang, SONG Li & XIE SiShen*

Beijing National Laboratory for Condensed Matter Physics, Institute of Physics, Chinese Academy of Sciences, Beijing 100190, China

Received September 1, 2011; accepted September 15, 2011; published online December 1, 2011

As a type of thin film, two dimensional (2D) reticulate architectures built of freestanding single-walled carbon nanotube (SWCNT) bundles are suitable for scalable integration into devices and nanocomposites for many applications. The superior properties of these films, such as optical transparency, unique electrical properties and mechanical flexibility, result not only from the outstanding properties of individual SWCNTs but also from the collective behavior of the individual tubes, with additional properties arising from the tube-tube interactions. In this review, the synthesis, structure and fundamental properties, such as conductivity, transparency, optical nonlinearity and mechanical performance, of "freestanding SWCNT bundle network" thin films and nanocomposites, as well as their application as supercapacitors are highlighted. Some long-standing problems and topics warranting further investigation in the near future are addressed.

single-walled carbon nanotube (SWCNT), SWCNT bundle network, nanocomposites, multifunctional thin film, supercapacitors

Citation: Zhou W Y, Ma W J, Niu Z Q, et al. Freestanding single-walled carbon nanotube bundle networks: Fabrication, properties and composites. Chin Sci Bull, 2012, 57: 205–224, doi: 10.1007/s11434-011-4878-0

As a kind of novel nano-structured material, carbon nanotubes (CNTs) have attracted intense attention owing to their marvelous mechanical, electrical, and thermal properties combined with low density, and also to their broad range of potential applications [1]. In comparison with multi-walled CNTs (MWCNTs), single-walled carbon nanotubes (SWCNTs) have shown more outstanding properties that benefit both nano- and macroscale applications of these materials with intriguing structure. An individual SWCNT can exhibit semiconducting or metallic or semimetallic behaviors, depending on its chirality and diameter [2]. Various types of SWCNTs are promising for advanced electrical interconnects owing to their low resistivities [3], high current-carrying capacities (up to ~10^9 A cm^{-2}) [4], and high thermal conductivities (up to 3500 W m^{-1} K^{-1}) [5]. The covalently bonded carbon network gives rise to an extremely stable structure, arguably the strongest in nature. The axial Young's modulus has been determined experimentally by several means [6–11] and is typically between 1–1.8 TPa. The fracture stresses of SWCNT bundles can reach as high as 50 GPa [8,12], which corresponds to a density-normalized strength ~50 times larger than that of steel wires [7]. In addition, the properties of SWCNTs are very sensitive to chemical modification or atomic doping — these processes can give rise to brand-new 1D materials that promise remarkable application. To fully utilize the excellent mechanical and physical properties of individual SWCNTs, various types of SWCNT architectures with different dimensions, including 1D nanotubes or bundles, 2D thin films or networks or papers, and 3D arrays or sponges, have been synthesized and investigated worldwide.

Unlike an isolated 1D nanotube, a 2D thin film made up of thousands of SWCNTs exhibits collective behavior, which has an advantage of statistically better reproducibility, making it suitable for scalable integration into devices, nanocomposites and for many applications. Its superior properties, such as optical transparency, unique electric properties and mechanical flexibility, result not only from

*Corresponding authors (email: wyzhou@iphy.ac.cn; ssxie@iphy.ac.cn)

the outstanding properties of individual SWCNTs but also from the additional properties due to the tube-tube interactions; understanding and exploiting these interactions is an emerging research field. Major challenges yet to be resolved include the controlled fabrication of 2D SWCNT materials with good reproducibility, utilization of the excellent properties of individual SWCNTs at a macroscopic level and prediction or exploration of new properties endowed by the macroscopic SWCNT assemblies. Recently, a novel 2D architecture built of freestanding SWCNT bundles has been fabricated [13–16]. These 2D SWCNT thin films or networks could exhibit unique physical properties and enhanced device performance. For example, Skakalova et al. [17] measured and compared the electronic transport properties of individual SWCNTs/MWCNTs with those of thin and thick SWCNT networks, and they found that a semiconductor-metal transition behavior, modulated through thin barriers, occurred as the film thickness increased. Several earlier reviews have addressed some aspects of SWCNT thin films as ideal building blocks for new types of applications in mechanically flexible and stretchable, optically transparent electronic systems, and as two-dimensional carbon networks in mechanically reinforced composites [18–22].

In this review, the synthesis, structure and fundamental properties, such as conductivity, transparency, optical nonlinearity and mechanical performance, of these special thin films, "freestanding SWCNT bundle networks", and their nanocomposites as well as their application as supercapacitors are highlighted. Some long-standing problems and topics warranting further investigation in the near future are addressed.

1 Fabrication of freestanding SWCNT bundle networks

1.1 Post-treatment approach

Earlier, yet effective, post-treatment techniques involve depositing tubes from solution suspensions to form SWCNT thin films, so-called "bucky papers" [23–25]. Generally, for this kind of method, a comprehensive strategy, such as surfactant wrapping to form stable solutions of SWCNTs, a robust mechanism to remove them from solution, and suitable way to take the film off the filter membrane, should be considered. SWCNTs can be removed from solution by, e.g. vacuum-filtration or evaporation of solvent [24,25] or specific interactions between nanotubes, ligands, and surfaces [26–31]. Owing to their cost efficiency, applicability to large areas and compatibility with a variety of substrates, solution deposition methods can be adopted for applications in transparent conductive coatings. However, an obvious limitation of the solution deposition methods is that it is difficult to obtain sub-monolayer or uniform thin SWCNT films without the presence of bundles. For this reason, some more effective solution methods have been developed, such as Langmuir-Blodgett techniques [32–34], dip coating [35,36], spray coating [37,38], spin coating [38– 40], solution casting by controlled flocculation process [41] and modified vacuum filtration [42– 44], to fabricate uniform large area films and to provide some patterning and/or alignment capability.

Recently, a simple "wet-transfer" approach [15] was proposed for preparing freestanding highly conductive transparent SWCNT films with 20–150 nm thickness by spray coating from surfactant-dispersed aqueous solutions of SWCNTs. After HNO_3 treatment, dipping the SWCNT films (supported on glass substrates) in water resulted in a quick and nondestructive self-release to form freestanding ultrathin SWCNT films on the water surface. The obtained films have sufficiently high transmittance (i.e., 95%), a very low sheet resistance (i.e., ~120 Ω sq^{-1}), and a small average surface roughness (i.e., ~3.5 nm for a displayed 10 μm × 10 μm area). Furthermore, the floating SWCNT films (F-SWCNT films) on the water surface could be easily transferred to any substrates of interest and preserve their original sizes and network structures. However, without the HNO_3-treatment, the F-SWCNT films were not released from the substrate surfaces, even when immersed in water for months. It is clear that the HNO_3 treatment sufficiently weakened the adhesion of the SWCNTs to the substrate surfaces. Nevertheless, special care should be taken when choosing the HNO_3 concentration.

Though almost all SWCNT films can be fabricated by the above-mentioned post-treatment, solution-based processes at room temperature, using tubes prepared by bulk synthesis procedures, and these processes are compatible with patterning techniques such as thermal, piezoelectric, or electrohydrodynamic jet printing [45–47], the relatively low strength of these films is one of the problems for their applications. Moreover, the SWCNTs must be first dispersed in solution suspensions, usually by means of high-power ultrasonication and strong-acid treatment, which may break the tubes and affect the electrical properties. In addition, the surfactant coatings may introduce some organic contaminants, which are unwanted for electronic devices. The development of more flexible approaches without solubilization seems desirable to solve these problems.

For example, to overcome the limit of the solution-based techniques in the choice of wettability of the substrates for applications, certain techniques, such as "dry-transfer", to relocate the SWCNT films from the deposited substrates to the target substrates of interest have been established [18–20]. One of the most successful post-treatment techniques is the "dry-drawing" approach [48,49], which provides a simple and natural way to obtain pure MWCNT yarns or films at a macro-scale and enables easy manipulation of nano-scale CNTs based on a superaligned CNT array. The best result achieved so far was the controlled synthesis of superaligned triple-walled CNT arrays [48]. This kind of

freestanding film will not be addressed in this review, since there are still challenges in synthesizing superaligned SWCNT arrays.

1.2 Direct synthesis

As one of the most popular synthesis methods, chemical vapor deposition (CVD) is not only an effective way to mass-prepare carbon nanotubes but also provides for direct growth of SWCNT films, although it is not as convenient for large-area substrates as the solution approaches. The main advantages of CVD are that the directly formed SWCNT films can be free of organic solvent contaminants and have high purity, controllable tube lengths, good crystallinity, and fewer tube bundles, as compared to those prepared by some solution-based techniques. Many strategies can be exploited to control the tube morphology (i.e., number of tube layers, diameter, length, geometrical shape, heterostructure), density (such as film thickness, pore volume of network and surface area), alignment or orientation, position, and so on. Many factors in CVD can affect the film morphology and its properties, e.g., the carbon source, catalyst, carrier gas, growth rate, substrate, template, external field, and so on.

Systematic studies have revealed that the carbon source is of crucial importance. Dai et al. [50] prepared SWCNTs using Mo as catalyst and carbon monoxide as carbon source. Later, they also used CH_4 as the carbon source and various catalysts [51–53]. Since CH_4 is the most stable of all hydrocarbons and does not easily decompose at high temperature, SWCNTs without amorphous carbon can be obtained [54]. With ethanol as the carbon feedstock, the film density can be increased significantly, compared to the case of methane, possibly because of the ability of OH radicals to remove seeds of amorphous carbon from catalytic sites in the early stages of growth [55,56].

A marked difference between the syntheses of SWCNTs and MWCNTs is that some catalysts are required for the former. High yield and good quality can be achieved by optimizing the catalyst and synthesis parameters [57]. Using Fe/Mo as bi-catalyst and an Al_2O_3/SiO_2 substrate, the growth of SWCNTs can proceed quite efficiently. Liu et al. [58] further optimized the technique and used the more active Fe/Mo/alumina (prepared by the sol-gel approach) as catalyst, and they achieved high yields by CVD. Cheng et al. [59,60] first applied the floating catalysis approach to synthesize SWCNTs and suggested it as a flexible way for high yield production. Other groups subsequently adopted this technique and optimized the carbon source for higher efficiency [52,61]. In particular, Smalley's group [62] used CO as the carbon source and produced large quantities of SWCNTs under a high pressure atmosphere. Their method is now known as the HiP_{CO} (high-pressure CO) approach, and has been widely applied to commercial production of SWCNTs.

In view of their selectivity towards the substrate and catalyst, SWCNTs can be controlled to grow at specific positions, assisted by microfabrication [63–65]. With respect to the fabrication of orientated SWCNTs aided by external fields, Liu and his collaborators [66] successfully realized the oriented growth of relatively long SWCNTs by controlling the gas flow with the floating catalysis approach. Furthermore, by applying an electric field during growth, an excellently oriented SWCNT array was fabricated between the electrodes on the quartz substrate [67–70].

Iijima's group [71] successfully fabricated a SWCNT array array, 2.5 cm in height, by introducing some water vapor into the system during CVD growth to maintain the activity of the catalysts and to extend their active lifetime. Very recently, Maruyama's group [72] further demonstrated experimentally that addition of H_2O during the supergrowth of SWCNT carpets could inhibit Ostwald ripening because of the ability of oxygen and hydroxyl species to reduce the diffusion rates of catalyst atoms. In addition, several groups reported arrays of individual SWCNTs with perfect linear shapes in horizontal configurations with high levels of alignment by optimizing CVD procedures [73–76]. Different means of transferring high quality CVD SWCNT films from growth substrates to other substrates, including flexible plastic sheets, have been established, thereby expanding their applicability [18,77].

However, the products synthesized by the direct processes are mainly powder-like and supported on different substrates. To directly prepare macroscale freestanding SWCNT films with high strength remains a challenging issue. Xie's group [13] reported a kind of thin film, the SWCNT non-woven film, synthesized directly by developing a floating catalyst CVD (FCCVD) system, in which the nanotubes are grown in a flowing gaseous feedstock mixture and form a piece of non-woven nanotube film on the wall of the quartz tube. After growth, the film can be easily peeled off. To directly synthesize high strength, highly conducting and transparent films, they further optimized the FCCVD growth parameters, such as the temperature of the catalyst source and the flux of the gaseous feedstock mixture [70,78–81], and adjusted the growth rate of the films as determined by the sublimation rate of the catalysts [82]. Freestanding SWCNT films of various thicknesses (100 nm to 1 μm), with areas up to several tens of square centimeters, were obtained. Under typical conditions, a 100 nm thick film will form after 30 min growth in the high-temperature zone and can be carefully peeled off a quartz substrate [16]. This type of large-area freestanding film can be easily handled for further studies. Furthermore, to overcome the limitation of this type of direct synthesis procedures with respect to the thickness (since the films should have a certain thickness to provide mechanical integrity) and the scalability of the as-grown nanotube film, they have developed a two-stage process for processing freestanding SWCNT films to resolve the stickiness problem and spread them out

onto various substrates uniformly, and obtained super-thin films with a thickness about 13 nm on a PET substrate [83].

The most recent improvement has been reported by Nasibulin et al. [84]. They reported a simple two-step method for the rapid fabrication of thin freestanding SWCNT films by dry transferring the collected nanotubes, directly grown on microporous filters, to a substrate. The films, with variable thicknesses ranging from submonolayer to a few micrometers depending on the collection time, have outstanding properties for several high-impact application areas: high efficiency nanoparticle filters with a figure of merit of 147 Pa^{-1}, transparent and conductive electrodes with a sheet resistance of 84 Ω sq^{-1} and a transmittance of 90%, electrochemical sensors with extremely low detection limits below 100 nM, and polymer-free saturable absorbers for ultrafast femtosecond lasers.

Another direct method to synthesize continuous SWCNT films is the arc discharge technique, which has been seldom used to grow SWCNT thin films directly. Ando et al. [14] produced SWCNT web by the DC arc discharge technique performed under a mixture of H_2 and Ar with a total pressure of 200 torr and achieved SWCNT films as thin as 30 nm, which could be peeled off the graphite plate without destroying the crystallinity and homogeneity of the as-grown film. For a 150 nm thick film, the measured transmittance was 77% [85].

Recently, Windle's group [86] reported a simple, single-stage, scalable method for the continuous production of high-quality carbon nanotube-polymer transparent conductive films from carbon feedstock by CVD. This method can adjust the concentration of nanotubes in the films by controlling the technical parameters, and scale up to prepare thin flexible composite films for any desired application, ranging from solar cells to flat panel displays.

2 Structural characteristics

SWCNT thin films form quasi-two-dimensional (2D) or three-dimensional (3D) interconnected networks of quantum wires, ranging from sub-monolayer to a few layers thick. The structure characteristics (conjunction between tubes or bundles) and properties (such as flexibility and conductivity) of the films are significantly affected by many factors, for instance, the distribution of orientation (i.e. tangle or alignment), density (tube number per unit area for thin random networks, tubes per length for arrays or layers for multilayer films), interconnection degree (for 2D planar or 3D spatial arrangement), and other aspects under the influence of an external field.

The SWCNTs in the reported "bucky paper" underwent post-treatment purification [23]: first a long period of refluxing in an acid, and then repeated re-suspension of the sediment in deionized water, centrifuging and decanting the supernatant liquid several times, and finally vacuum filtering off the liquid through a porous membrane. In the as-obtained mat, the SWCNTs have a short length (several microns) and weak interconnections with each other, so it is difficult to transfer them from the membrane, since the mat is rather brittle. Only a sufficiently thick SWCNT layer may be readily peeled off the membrane to produce a freestanding mat.

In 2000, Smith et al. [87] produced thick films and ropes of aligned SWCNTs by filtration/deposition from suspension in strong magnetic fields. Since tubes and ropes in suspension adopt a preferred orientation with their axis parallel to the applied field and the ropes in ordinary "bucky paper" lie preferentially in the plane of the film, a magnetic field applied during filter deposition introduces a preferred direction in the plane. They found that aligned films are denser than ordinary filter-deposited ones, and much denser than as-grown material. However, because of lack of transverse (i.e. radial) conjunction between tubes or bundles, the aligned film cannot be transferred in large areas from the membrane. The films peeled away from the filter are usually in the form of long narrow strips parallel to the field direction, a consequence of the rope alignment.

Therefore, the formation of a freestanding thin film depends on the extent of conjunction between tubes or bundles, which reflects the distribution of orientation and density of the film. It seems that the more random the arrangement of tubes or bundles in a film, the greater the density of SWCNT-SWCNT junctions, and the easier formation of a continuous thin film. Several scaling laws, with respect to film density, thickness, width, tube length, tube wall number, and bundle diameter, have been applied to predict whether the thin film is continuous [20]. Moreover, for a freestanding thin film, the strength of the SWCNT-SWCNT junctions in the film must be a dominating factor; and for a transparent film especially, other factors which influence the impurities and homogeneity must be considered, in addition to the density and strength.

To obtain high-quality transparent films, several crucial improvements have been made by Xie's group [16], to control the density, impurities, and homogeneity of the prepared thin films: (i) the density and the growth rates were well controlled by precisely adjusting the sublimation rates of the catalysts; (ii) the impurities in the as-grown films were further reduced, compared to their earlier results; (iii) the homogeneity of the films was ensured by the use of specially stabilized gas flow in the quartz tube. As seen in Figure 1(a) and (b), the homogeneity of the film is good enough in a typical 5 cm × 10 cm area to permit optical transparency. If the films are not very homogeneous, they will lose their transparency because of severe diffusion even if they are thin enough (Figure 1(c)). Figure 1(d) is a SEM image of a 250 nm thick as-grown film, and shows that the SWCNT bundles are homogeneously distributed, entangled with each other, and of low-level impurities. The SWCNT thin film is composed of highly entangled carbon nanotube

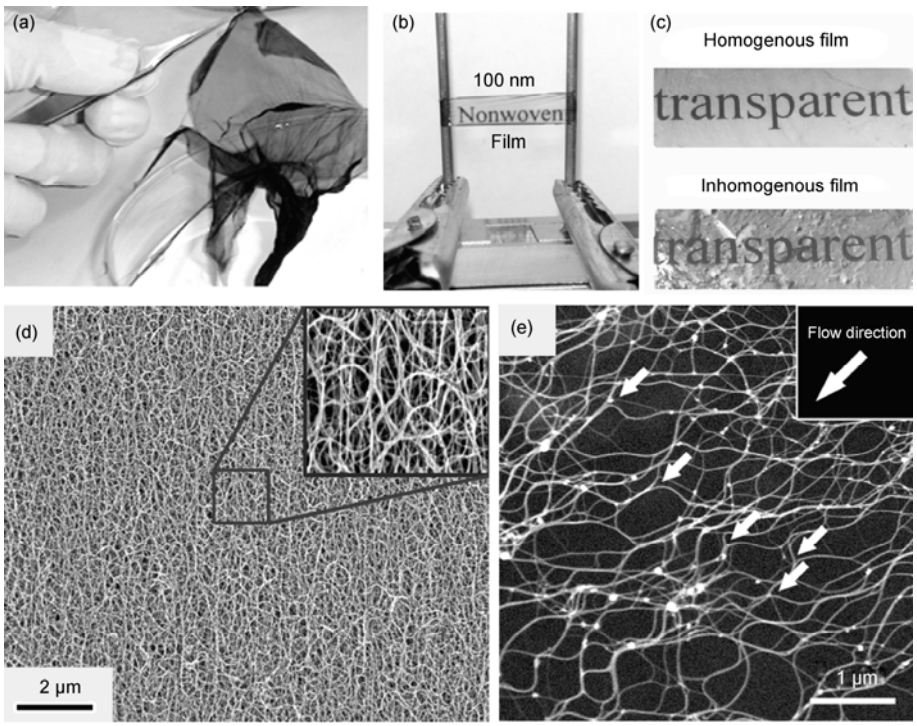

Figure 1 (a) Photograph of an as-grown 250 nm thick SWCNT non-woven film. (b) A transparent 100 nm thick film freely stands between metallic pillars. (c) The 150 nm thick homogeneous and inhomogeneous films. The importance of homogeneity is clear. (d) Large-scale scanning electron microscopy (SEM) image of a 250 nm thick film. The inset image is taken at higher magnification. (e) SEM image of SWCNT network in a single layer. The white arrows in the image denote the Y-type junctions and the flow direction. Reproduced with permission from ref. [16].

bundles about 30 nm in diameter and from tens to hundreds of microns in length. The diameter of the nanotubes in the bundles is about 1–2 nm. It is emphasized that the bundles in the films firmly connect via Y-type junctions with each other when they are growing and form a continuous, preferentially oriented, 2D network at high temperature (Figure 1(e)), which is a crucial factor for making the ultrathin film freestanding and for manifesting its unique electrical properties and mechanical flexibility, as discussed below.

3 Properties of freestanding SWCNT bundle networks

In contrast to the isolated tube, thin films of SWCNTs are suitable for scalable integration into devices, owing to their superior optical transparency, unique electrical properties and mechanical flexibility. These superior properties benefit not only from the individual SWCNTs but also from the collective behavior of the individual tubes because of the tube-tube interactions. In several earlier reviews [18–20], SWCNT thin films have been introduced as ideal building blocks for new types of applications in mechanically flexible and stretchable, optically transparent electronic systems, and as two-dimensional carbon networks in mechanically reinforced composites. Here some of the fundamental properties, such as conductivity, transparency, optical nonlinearity and mechanical strength, of freestanding thin SWCNT films are addressed.

3.1 Transparency and electrical conductivity

SWCNT thin films are quasi-2D interconnected networks of quantum wires. The electrical conductivity of the films should be composed of the intrinsic conductivity of individual nanotubes within the network and that associated with the junctions between SWCNTs or their bundles, which is strongly influenced by many factors. In addition to some obvious factors, such as the doping level of the semiconducting tubes, sample purity, and the metallic-to-semiconducting volume fraction (raw SWCNTs are, generally, a mixture of m- and s-SWCNT in a ratio of 1∶2 statistically [88]), the structural characteristics of the bundles, for example, the geometry (length, diameter, junction shape), the distribution (orientation, spatial arrangement), and the density, have a prominent influence on the network conductivity. These factors also affect the transparency of the films, as discussed in detail in many review articles [18,19,21]. Here, the focus will be only on the structural effect on transparency and electrical conductivity of freestanding random SWCNT networks.

Although the axial conductivity of a SWCNT rope can reach 10000–30000 S cm^{-1} [89], the conductivity in films or networks is usually 1 or 2 orders of magnitude lower. For

random SWCNT networks, an electrical conductivity ranging from 400–6600 S cm^{-1} has been reported [90,91]. Purifying or compacting of the films has proved favorable for increasing the conductivity to a certain extent [23,90]. These results demonstrate that the conductivity is dominated by the intertube junctions. Clearly, the density of bundles in the random SWCNT networks consisting of a mixture of m- and s-SWCNTs has a more pronounced effect on the transparency [17,92,93]. Opaque mats (i.e., "bucky papers'') have nanotube densities far exceeding the percolation threshold and are unsuitable for solar applications where transparency is critical [23]. As the film thickness increases, the film loses transmittance through absorption. Therefore, to maximize the potential use of SWCNT networks as transparent conductors, it is desirable to have a low sheet resistance and a high optical transmittance. An approximate relationship between sheet resistance (R_s), optical transmittance (T), DC conductivity (σ_{dc}), and optical conductivity (σ_{op}), is given by the following formula [25]:

$$T=\left(1+\frac{1}{2R_s}\sqrt{\frac{\mu_0}{\varepsilon_0}}\frac{\sigma_{op}}{\sigma_{dc}}\right)^{-2}=\left(1+\frac{188(\Omega)}{R_s}\frac{\sigma_{op}}{\sigma_{dc}}\right)^{-2}, \quad (1)$$

which is valid for thin metal films where the absorption of the material is much smaller than the reflectance, and the thickness of the film is much less than the wavelength of interest. Another commonly used quantity for characterizing the performance of transparent conductors is the figure of merit, defined as T^{10}/R_s [19,94].

Ma et al. [16] systematically studied the transmittance spectra ranging from ultraviolet to mid-infrared and the sheet resistance of as-grown freestanding uniform SWCNT films with different thicknesses (Figure 2(a) and (b)). For a 100 nm thick film with a sheet resistance of 50 Ω sq^{-1}, which was the thinnest intact film they could peel off the wall of the quartz tube, the transmittance in the visible region of the spectrum was over 70% when coated on a substrate. In comparison with films made from a solution-based filtration process, the directly synthesized films have superior electrical and mechanical properties: the electrical conductivity can reach over 2000 S cm^{-1} and the strength can be as high as 360 MPa. These intriguing properties are believed to result from the good and long interbundle connections, as shown in Figure 1(e). Hone et al. [95] ascribed the high conductivity to the unique structure of the films: (i) The bundles in the films were not randomly distributed but preferentially aligned by the flow whilst they were growing in the reaction zone. Because of this anisotropic strength, all the films suspended between two metallic pillars were mounted along the preferential direction, which effectively enhances the conductivity, as previously revealed. (ii) The bundles in the films firmly connect with each other during growth, and form a continuous preferential 2D web at high temperature, whereas in the films made by filtration, the contacts are weak and sometimes blocked by amorphous carbon. In fact, the bonding at the junction parts is so strong in the directly synthesized films that, when it is attempted to disperse the tubes in acetone, the films remain intact even after hours of ultrasonication. Up until now, although many techniques have been developed to treat SWCNTs, there are only a few reports on how to improve the electrical contacts between bundles. It is demonstrated that connecting bundles into a continuous net whilst they are growing is an effective way to obtain better contacts and to lower sheet resistance [16].

These flexible, transparent, freestanding SWCNT films can be easily transferred to various substrates, which should broaden their application prospects. To enhance the transparence of as-prepared SWCNT films, Niu [83] presented a novel strategy, "repeated transfer-printing", for the post-treatment of the directly grown freestanding SWCNT films, to fabricate ultrathin films on a flexible and transparent substrate. The thinnest film had a thickness of 13 nm and a transparency of over 90%. Recently, by a simple single-stage and scalable method, Windle's group [86] have prepared high-quality carbon nanotube-polymer transparent conductive films. Their best results show a surface resistivity of the order of 300 Ω sq^{-1} for a film with 80% transparency,

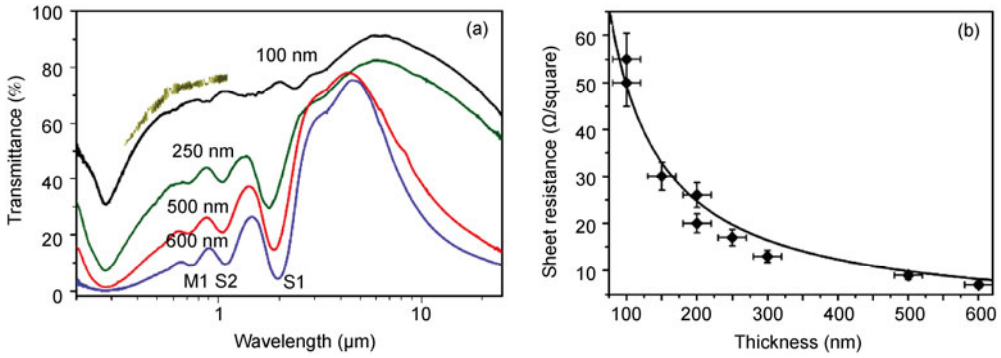

Figure 2 (Color online) (a) Transmittance spectra of as-grown films with different thicknesses. The numbers above the curves denote the thicknesses, and the uppermost short curve corresponds to the 100 nm thick film on a glass substrate. S1 and S2 represent the electronic transitions for the semiconducting SWCNTs in the films, and M1 represents that of the metallic nanotubes. (b) Sheet resistance versus thickness of SWCNT films. The solid line is the best fitted curve according to the definition of electrical conductivity. Reproduced with permission from ref. [16].

achieved by adjusting the concentration of nanotubes in the films.

As promising candidates for transparent conductors on account of their intrinsic mobility of over 100000 cm^2 V^{-1} s^{-1} [96], good mechanical flexibility [97], and good optical transparency [98–100], SWCNTs have been studied extensively for their possible application in field-effect transistors [90,100–102], touch-screens, liquid-crystal displays, solution-processed solar cells [103], and so forth. Most recently, Zhou and co-workers [104] reported high-performance, fully transparent thin-film transistors (TTFTs) on both rigid and flexible substrates with aligned nanotubes as an active channel. Transparent transistors with high effective mobilities (~1300 cm^2 V^{-1} s^{-1}) were first demonstrated on glass substrates via engineering of the source and drain contacts, and a high on/off ratio (3×10^4) was achieved using electrical breakdown.

Nevertheless, a detailed understanding of the control of the overall optical and transport properties of transparent SWCNT thin films has not yet emerged because of its complexity. In fact, it is not yet ascertained which kind of film is a better transparent conductor, one formed solely with m-SWCNTs or solely with s-SWCNTs. At first sight, we might anticipate that metals would be better for conductivity in the films, while semiconductors would be better for transparency. However, choosing the best composition to optimize both characteristics simultaneously is difficult. Recently, Blackburn et al. [105] systematically investigated the optical and electrical properties of transparent conductive films with precisely tuned ratios of metallic and semiconducting SWCNTs. They found that the conductivity and transparency of the films were determined by an interplay between localized and delocalized carriers, which depends upon the SWCNT electronic structure and tube-tube junctions as well as intentional and unintentional redox dopants.

3.2 Third-order optical nonlinearity

SWCNTs are direct-bandgap materials with a gap depending on diameter and chirality [106]. Theoretical and experimental studies have shown that CNTs are strongly nonlinear media [107–109], since the delocalization of π electrons has been shown to be a major contribution to the large off-resonant third-order optical susceptibility. A CNT is a highly delocalized π-conjugated electron system. The fast nonlinear optical response may be due to the large polarization arising mainly from the π–π^* virtual transitions [108,110].

Most studies have focused on theoretical modeling of nonlinear optical properties of CNTs utilizing the perturbative approach with the polarization of the medium being represented by a power expansion in the electric field strength, truncated to a certain term (usually the third term). In this case, the nonlinear response of CNT-based composites is characterized by the cubic susceptibility which describes a variety of nonlinear effects, such as self-phase modulation, self-focusing and self-defocusing, four-wave mixing, and third-order harmonic generation. Nemilentsau et al. [110] elaborated a non-perturbative time-domain analysis of the high-order harmonic generation in CNTs and presented a consistent quantum-mechanical approach to nonlinear optics of CNTs. They studied the nonlinear interaction of an isolated CNT with femtosecond laser pulses in the vicinity of plasma resonance, based on a quantum-mechanical description of π-electrons taking into account both intra-band and direct inter-band transitions.

In 1999, the third-order optical nonlinearity of multi-walled CNT solutions was studied using a backward degenerate four-wave mixing (DFWM) technique, pioneered by Liu et al. [108,111]. Subsequently, a series of experimental work have been reported [109,112,113]. Chen et al. [112], using a pump-probe method with a 150 fs laser at a wavelength of 1.55 μm, demonstrated that SWCNTs have an exciton decay time of less than 1 ps and a high third-order polarizability in a polyimide-SWCNT composite film with thickness of about 20 μm and a SWCNT loading of less than 0.1 wt%, which was reasonably interpreted to be because of their azimuthal symmetry. Tatsuura et al. [114], using semiconducting carbon nanotubes as ultrafast switching materials for optical telecommunications, observed that spray-coated SWCNT films exhibited a very useful combination of high nonlinear optical properties $\chi^{(3)}$ close to the order of 10^{-7} esu, high linear absorption coefficient α_0, and fast response time in the infrared region. By the Z-scan method, Maeda et al. [113] measured the third-order nonlinear susceptibility ($\chi^{(3)}$) spectra of semiconducting SWCNT thin films, which were prepared by spraying SWCNTs suspended in ethanol under sonication on CaF_2 substrates. They confirmed that $|\mathrm{Im}\chi^{(3)}|$ is remarkably enhanced under resonant excitation of the lowest interband transition, reaching 4.2×10^{-6} esu and 1.5×10^{-7} esu in SWCNTs grown by the laser ablation and HiPco methods, respectively. A comparison of the transient absorption changes evaluated by degenerate and nondegenerate pump-probe measurements suggests that the resonant enhancement of $|\mathrm{Im}\chi^{(3)}|$ is dominated by a coherent process rather than by saturation of absorption. These experimental results reveal that semiconducting SWCNTs, as well as their polymer composites, have potential applications in optical telecommunication devices, for instance as candidate materials for high-quality sub-picosecond all-optical switches, with high performance, low production cost, low toxicity, and high environmental friendliness.

Compared with solution-deposited SWCNT films, directly synthesized freestanding SWCNT films have superior hierarchical structure, which would facilitate the relaxation of carriers, effectively reduce the total optical loss, and enhance the output power of mode-lock lasers. Long et al. [115] investigated the carrier dynamics of SWCNT films in a degenerate pump-probe experiment at 1.57 eV. They

measured ultrafast time-resolved optical transmission in SWCNTs as a function of pump fluence at a temperature of 200 K, and observed relaxation dynamics with two components characterized by time scales of 0.1 and 1 ps, respectively. It is suggested that the fast component is related to the intraband relaxation and the slow component to two competing processes, since the signal amplitude shows a crossover from negative to positive when the pump fluence is decreased. Ma et al. [116] investigated the nonlinear optical properties of directly synthesized freestanding SWCNT films. Large third-order optical nonlinearity was observed by the Z-scan method. The third-order nonlinear susceptibility ($\chi^{(3)}$) was measured, and the $|\mathrm{Im}\chi^{(3)}|$ was 1.8×10^{-7} esu at 1064 nm, which is among the highest values for optical nonlinear materials. Transparent SWCNT/epoxy composite films were also fabricated, where epoxy resin was introduced to protect the SWCNTs from ablation under strong light. Combined with their ultrafast carrier relaxation times, the results indicate that these as-prepared transparent films are excellent candidates as saturable absorbers for use in mode-lock lasers, or as ultrafast switching materials in optical telecommunications, because of their sub-picosecond recovery time, low saturation intensity, polarization insensitivity, and mechanical and environmental robustness.

Recently, Wang et al. [117] engineered a SWCNT-polycarbonate film with a wide bandwidth around 1.55 μm as a passive optical switch, and then used it to demonstrate a 2.4 ps Er^{3+}-doped fiber laser that is tuneable from 1518 to 1558 nm. So, a prototype of mode-locking fiber laser based on SWCNT saturable absorbers with wideband tuneability, instead of traditional semiconductor saturable absorber mirrors, has been successfully produced. Their work makes use of SWCNTs with a range of diameters and chiralities, harnessing the resulting wideband absorption to produce a wideband-tuneable fiber laser, and turning a major disadvantage of SWCNTs for applications in nanoelectronics into an advantage.

3.3 Mechanical properties and micromechanical analysis

CNTs have been envisioned as ideal building blocks for high-performance engineering materials, owing to their promising mechanical properties and low density. Theoretical and experimental work on the mechanical properties of individual or bundles of CNTs has been conducted extensively since the end of the last century [8,118,119]. It turns out that the modulus and strength of a typical SWCNT can reach 640 and 37 GPa, respectively, which surpass those of all existing materials [120]. However, because of weak intertube interactions, it is still a great challenge to retain such supermechanical properties when CNTs are assembled into macroarchitectures (such as fibers and films).

For example, despite the high stiffness and strength of individual SWCNTs, slips between nanotube surfaces hinder the application of SWCNT bundles as a reinforcing material in composites [8]. To resolve the "slipping problem", several methods have been proposed, such as reducing the bundle diameters [8,121], bridging adjacent tubes by electron-beam irradiation [122], and prolonging the contact length between tubes [123], but none has been proven feasible at the macroscale. Directly synthesized strong films with simple and uniform structure offer an alternative, since the as-grown SWCNT networks have a preferentially oriented and firmly connected reticulate architecture (Figure 1(e)) [16], which can provide continuous load-transfer pathways. For a 200 nm thick film, the tensile strength is 300–400 MPa (Figure 3(b)) [124], which is 30 times higher than that of typical "bucky paper" and 10 times higher than that of sheets with nitric acid treatment [125]. The density-normalized stress is 280 MPa g^{-1} cm^3, which is higher than that of undensified MWCNT sheets drawn from nanotube arrays but lower than that of densified MWCNT sheets [49]. The Young's modulus is about 5 GPa. Compared with the theoretical strength of individual SWNT (37 GPa), the film

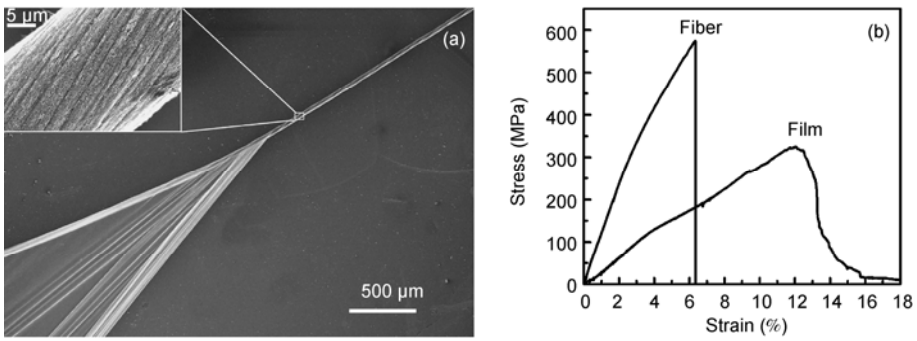

Figure 3 (a) The SEM image shows a piece of as-grown film with a width of 2 mm and a thickness of 200 nm being twisted into a fiber. It should be pointed out that, for the specimens prepared for tensile tests, there still is a densification procedure before twisting by immersing the films in acetone. This procedure effectively reduces the free volume in the fibers and is necessary for the later comparison of mechanical properties between fabricated fibers and films (whose thicknesses are measured after densification). (b) Typical strain-stress curves for the films and fibers. The fracture manner for the fiber becomes catastrophic. This is because the twisting structure blocks the bundles' free sliding and stores more mechanical energy; when a critical defect emerges, the released energy destroys the fiber rapidly. Reproduced with permission from ref. [124].

strength (~360 MPa) is two orders of magnitude smaller. That is because, similar to other engineering materials, the strength of macroscale SWCNTs is dominated by the stress transfer mechanism rather than by an individual SWCNT's strength.

In fact, poor load transfer arises not only from the weak intertube connections but also from the increasing possibility of failure when load is transferred through a long gauge length or a large cross-sectional area. Recently, Windle and co-workers [126] reported the synthesis of continuous high-performance CNT fibers with the highest measured strength of 9 GPa. They found that the tensile strength varied with the gauge length of the specimens: when the gauge length increased from 1 to 10 mm (typical for tensile tests), the average strength rapidly dropped to 1 GPa. Such degradation was attributed to a load transfer deficiency caused by local defects during densification. Up to now, the attention paid to this type of "negative" size effect seems insufficient. For example, the dimensions of specimens are often not mentioned when experimental results are reported, which makes systematic comparative studies difficult. Besides the size effect, the variety of CNT constructions in specific macrostructures, and the difficulty of accurately measuring the volume fraction of CNTs within fibers, also blur the evaluation of the related mechanical properties. Thus, we need a generic methodology, independent of mechanical measurements, to help us understand the inherent interbundle strength and microscopic failure processes for various CNT macro-architectures.

Ma et al. [124] have applied Raman tests to characterize the micromechanical process in strained SWCNT films and fibers. The down-shifting trend of the peak position and the asymmetrical broadening of the line shape after strain are the major characteristics of the Raman spectra for both types of specimens (Figure 4). The down-shifts of the G' band are expected and arise from the weakening of the carbon-carbon bonds as a result of the elongated interatomic distance. Asymmetrical G'-band line shapes under strain are uncommon and have not been reported for individual strained CNTs. Moreover, when more Raman measurements are performed under different strains (Figure 4(b)), the down-shifts of the G' band show two-stage behavior: at low strains, they increase linearly at rates of 0.65 (film) and 1.7 (fiber) cm^{-1} per 1% strain; once the strains exceed a

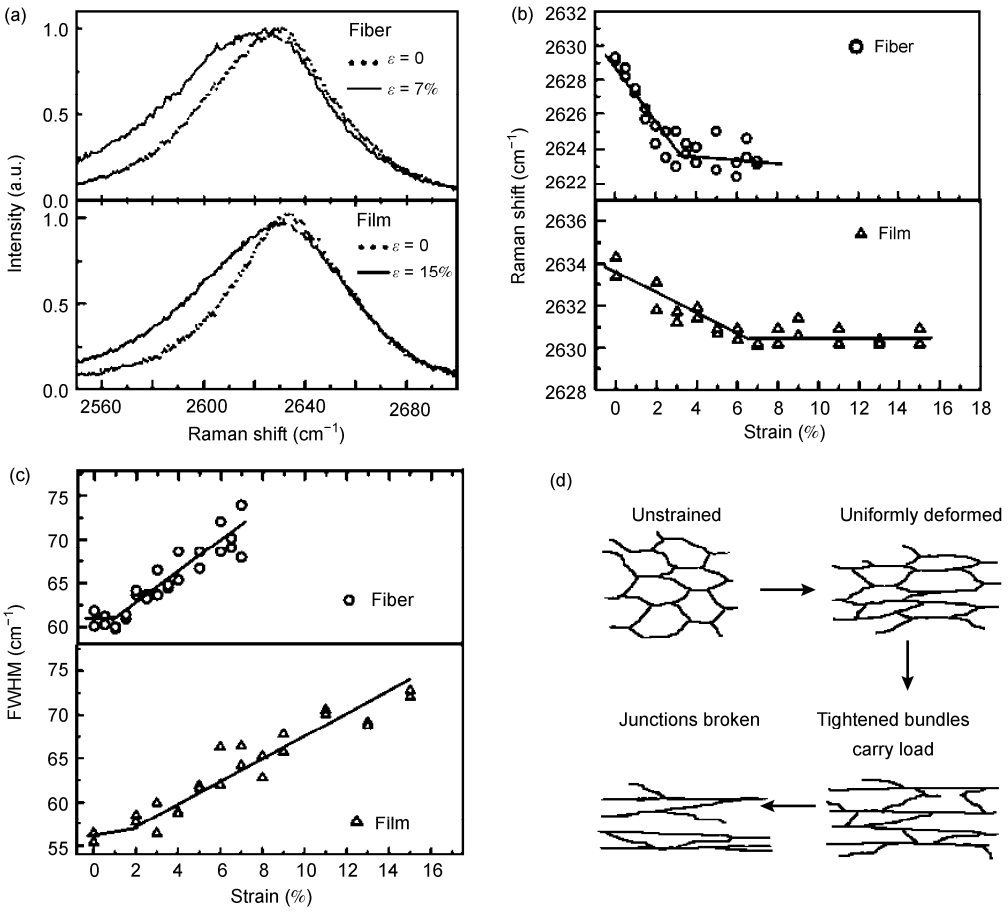

Figure 4 Typical G' band Raman spectra of a strained SWCNT film and fiber. (a) Comparison of the Raman spectra of unstrained and max-strained film and fiber. (b) The Raman shift of the G' band as a function of applied strain. (c) The widths of the G' band for a strained film and fiber. (d) A schematic image showing the deformation process for the SWCNT meshes in a film when macroscale strain is applied. The deformation process in the SWCNT fiber is similar except for the pre-elongation of the meshes as a result of the twisting process. Reproduced with permission from ref. [124].

certain value (6% for the film and 2.5% for the fiber), the peak position of the G' band changes little until final breakage of the specimens. According to Cronin's report [127], the average down-shift rate of the G' band for strained individual SWCNTs is 37.5 cm^{-1} per 1% strain, which is 56 times that of films, and 21 times greater than that of fibers. Such small down-shift rates for the strained SWCNT films and fibers imply that SWCNT axial extensions merely contribute a few percent to the total macroscale strain, which is consistent with the remarkable drop of the macroarchitecture moduli as compared to those of individual CNTs.

As shown in Figure 4, the changes in the Raman G' band spectra for the strained films and fibers are obviously different. In 2004, Baughman's group [128] improved Fan's array-spinning technique [129] and realized the importance of the twisting process for the synthesis of macroscale CNT fibers. They stated that the twisting of the nanotubes generated lateral force and gave rise to nanometer-scale friction force to couple these tens of micrometer long CNT bundles together as a continuous fiber. The enhancement effects of the twisted structures on the fibers' mechanical properties were also verified by some other researchers [130]. However, because of the shortage of samples and the limitation of macroscale tensile tests, we know little about how the friction law works at the nanometer level and how the parameters such as twist angle and twisting force influence the mechanical performance of these spun CNT fibers. Based on the Raman data, Ma et al. [124] have estimated the moduli of the films and fibers. The tensile tests confirm their conclusion from Raman measurements: the strengths of the fibers range from 550–800 MPa, in comparison with the values of 300–400 MPa for films (Figure 3(b)). They ascribed such strengthening of the interbundle junctions to the twisting-induced lateral stress in the fibers. Under this type of compressive stress, hollow SWCNTs are radially deformed, which generates more friction force to prevent intertube sliding as compared with undeformed nanotubes [123,130]. In addition, the long interbundle connections in the directly synthesized films ensure that the friction force can accumulate to a certain degree to block the free movement of the bundles [16]. This easy and effective methodology that they have developed, i.e., by investigating the variation of the Raman G' band under strain to infer the structural deformation process of the CNT fibers and further to predict the macrostructures' moduli, can be applied to other kinds of CNT macro-architectures as a valuable supplement to macroscale tensile tests for monitoring the mechanical process at the micrometer scale.

4 Nanocomposites based on freestanding SWCNT bundle networks

As a concept, "nanocomposites" arose in the 1990s with an increasing use of nanosized fillers such as nanoparticles and nanofibers. In the case of SWCNTs, the terms "nanocomposite" and "molecular composite" are roughly equivalent since the nano-filler consists of individual SWCNT molecules [131].

Besides the outstanding electrical and thermal properties, a SWCNT has a density of about 1.33–1.40 g cm^{-3}, which is just one-half the density of aluminum, whilst its elastic modulus is comparable to that of diamond (1.2 TPa). The tensile strength for SWCNT bundles is measured as 13–52 GPa [8], and has been calculated as 150 GPa for a single SWCNT [132], much higher than that of high-strength steel (2 GPa). It has been confirmed that the axial mechanical strength of SWCNTs approaches the theoretical value of a perfect graphite sheet and is the highest among all presently known materials [97], which makes SWCNTs promising building blocks for fabricating composite materials with excellent mechanical performance and unique electrical and thermal properties. With such attractive prospects, a great deal of effort has been made by many researchers over the past decade. Several reviews have focused on some aspects of SWCNTs as ideal building blocks for nanocomposites [97,131,133–136], while most reviews addressed composites of MWCNTs [134]. Since the axial tensile Young's modulus and shear modulus are sensitive to nanotube diameter and nanotube structure, here nanocomposites based on freestanding SWCNT bundle networks will be emphasized.

4.1 High-strength nanocomposites reinforced by freestanding SWCNT bundle networks

In spite of extensive studies on the mechanical properties of SWCNT reinforced nanocomposites [97,131,133,134], progress to date has been far behind expectation. The real potential of micro-scale SWCNTs has not yet been manifested in macro-scale materials. There are several daunting challenges: (1) Dispersion. SWCNTs tend to agglomerate, because of van der Waals interactions, their very large ratio of length to diameter, and their low surface energy. Uniform dispersion of SWCNTs is the critical issue, since at present a maximum of only 5 vol.% nanotubes can be dispersed uniformly in a polymer matrix. (2) Interface. Another major issue is the limited interfacial shear strength between SWCNTs (or SWCNT bundles) and the polymer matrix. (3) Waviness. A MWCNT with a diameter of 10 nm is 10^{12} times easier to bend than a carbon fiber with a diameter of 10 μm since the flexibility of a pillar-like structure is inversely proportional to the quartic power of its diameter. Therefore, like MWCNTs, SWCNTs are naturally extremely wavy, which significantly impairs their reinforcement effect [137]. (4) Slippage. Because of the atomically smooth surfaces of the CNTs, their bonds to the matrix are noncovalent if no chemical modification is applied to the walls of the CNTs, which results in ubiquitous interfacial slippages between SWCNT bundles or MWCNT walls when

local stress is increased to some extent [138]. Therefore, even if homogeneous dispersion is achieved, CNTs in composites actually carry a load much lower than that anticipated.

To overcome the challenges of macro-scale SWCNT structures and their composite materials, Xie et al. conducted a long-term and in-depth study. They were the first to fabricate macro-length SWCNT arrays [139] and measured their mechanical properties [11,13]. In recent years, they proposed that the mechanical properties and potential applications of macro-scale SWCNT films and fibers can be predicted using information from Raman spectra [124]. On the basis of this work they concluded that: for the recently developed nano-scale reinforced structures based on SWCNTs, new load-bearing and load-transferring structural units need to be designed. To obtain high-performance SWCNT reinforced composite materials, the keys are to improve the volume fraction and orientation of the tubes and to increase the interface strength. The traditional fabrication process of dispersing nanotubes directly into the polymer matrix, although simple, is not suitable for nano-scale reinforcement. Therefore, new methods are needed to fabricate this new type of material. For example, composites were synthesized based on macro-scale CVD-grown SWCNT thin films, with infiltration using thermoset epoxy resin or thermoplastic poly (vinyl alcohol) (PVA) as polymer matrices [140]. Figure 5 shows the morphology, schematic illustration and fracture mechanism as well as the tensile modulus and strength of SWCNT-reinforced composites. Most importantly, in this new continuous interpenetrating reticulate architecture with strong coupling at molecular-level, the volume fraction of SWCNTs may be controlled in the range of 30%–50%, which overcomes the limit of volume fraction in traditional approaches. The median strength of the epoxy-infiltrated fibers is as high as 1.6 GPa (Figure 5(d)), which is higher than that of continuous carbon fiber reinforced unidirectional tapes (T300/epoxy) with the same volume fraction of reinforcement. Compared with "bucky paper" based high-SWCNT-content composites, the tensile strength of this new composite is more than one order of magnitude higher. This result demonstrates that the true potential of CNTs (although not yet fully realized in this new composite), can be reached in composites as initially envisioned through load-transfer-favored three-dimensional architectures and molecular-level couplings with the polymer chains.

Further studies on the micro-mechanical processes led Xie et al. [140] to discover that the load transfer efficiency from the macro-strain of composites to the axial strain of SWCNTs in this composite was several times larger than that in discrete SWCNT reinforced composites prepared by conventional methods. They attributed this feature to the

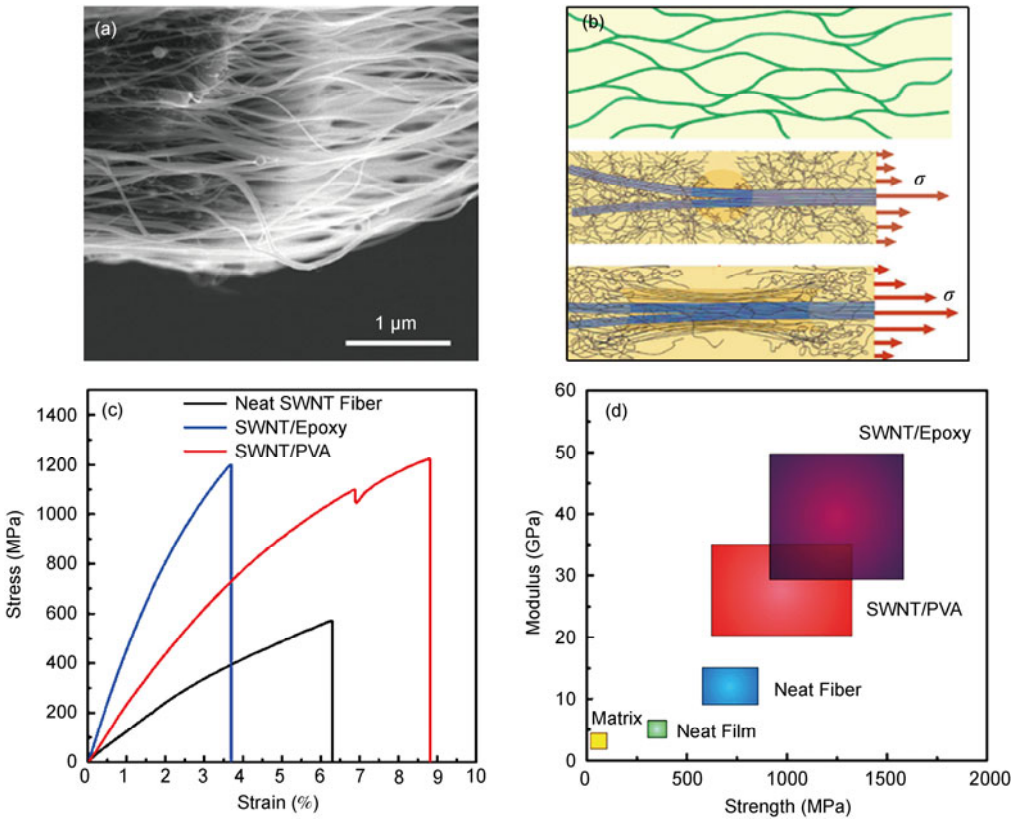

Figure 5 (a) Morphology of SWCNT-reinforced composites. (b) Schematic illustration and fracture mechanism of reticulate SWCNT reinforced composite fiber. (c) Typical tensile test results of composite fibers and neat SWCNT fibers. (d) Summary of the tensile modulus and strength for tested samples. Reproduced with permission from ref. [140].

strong molecular-level coupling between the polymer chain segments and the carbon nanotube bundles. The coupling varies with the molecular structure of the polymer used, and the simple mixing rules used in the field of traditional composite materials cannot describe this molecular-scale coupling. A schematic illustration and fracture mechanism of reticulate SWCNT reinforced composite fiber are shown in Figure 5(b). Based on these discoveries, they introduced an extra factor, the strain-transfer-factor (STF), into the general mixing theory and put forward a new mixing rule suitable for SWCNT reinforced composite materials, by which the macro-scale mechanical properties affected by molecular-level coupling between the polymer chain segments and the bundles are well described. Their results not only solve the problem in the preparation and improvement of SWCNT reinforced composite materials, but are also beneficial in studies of other nanocomposites [133].

4.2 High-conductivity nanocomposites improved by adding freestanding SWCNT bundle networks

The wide use of nanocomposites is essentially owing to the improvement in mechanical properties as a result of filling a host material with some reinforcing nanofillers. If the reinforcing component is electrically conductive, it may form a percolating network within the matrix at a specific volume ratio, which will result in a remarkable increase in the conductivity of the composite [141,142]. Therefore, measurements of electrical conductivity are important not only for characterizing the electrical properties of the composite but also for measuring the dispersion quality. Li and Chou et al. [143,144] systematically examined the factors contributing to electrical conductivity of nanocomposites and carried out a Monte Carlo simulation of the percolation threshold from a probabilistic viewpoint. The following issues are include in their resistivity modeling: the identification of filler contact status, establishment of wavy nanotube network, determination of percolation threshold, identification of spanning clusters and backbone, contact resistance modeling as well as the resistivity and damage modeling of CNT/fiber hybrid composites. The nanocomposites reinforced by the directly synthesized SWCNT bundle networks, which always contain a "closed circuit" as described in Section 2 and Section 3.1, have superior electrical properties in addition to their outstanding mechanical performance. Song et al. [145] prepared sandwich-like SWCNT paper/PEEK nanocomposites with good interfacial adhesion by a simple hot-pressing method. One layer of SWCNT paper gave the best results under their process conditions, i.e., ~40% and 4% increases in Young's modulus and failure strength, respectively. Moreover, the surface electrical conductivity increased sharply after loading the SWCNT paper onto the surface of the PEEK matrix, because of the good intrinsic conducting property of the SWCNT. The thermal conductivity of the matrix was also slightly improved.

Thin transparent SWCNT films and their reinforced nanocomposite films have received increasing attention as replacement conductive materials and emerge as promising candidates for transparent electronics and optoelectronics [15,19,44,146,147], owing to their attractive electrical, optical, and mechanical properties and their stretchability and chemical stability [9,18]. Encouraging progress has been made in scaling-up their fabrication and application. For example, Windle's group [86] reported a single-step continuous process based on CVD that produces transparent and conductive nanotube-polymer films. The single-step approach avoids the difficulty in achieving stable CNT suspensions. The films are mechanically robust once they are cast onto a polymer substrate and neither flexing nor bending reduces their electrical conductivity. Transparent conductors manifest wide applications from lighting, touch panels, displays, and photovoltaics to smart windows and EMI shielding.

Rogers et al. have fabricated high-performance "all-SWCNT"-constructed flexible, transparent thin film transistors (TFTs), using CNT networks as source/drain/gate electrodes as well as the semiconducting channel. The TFTs exhibit an effective mobility ~30 $cm^2\ V^{-1}\ s^{-1}$ and high mechanical stretchability (<3.5%) [100]. Owing to the relatively high work function of SWCNT films (~4.9 eV) [148], they can serve as anodes for hole-injection/extraction in several types of photonic devices, such as organic light-emitting diodes (OLEDs) and organic solar cells [149,150]. It has been demonstrated that the luminescence, turn-on voltages, and power efficiencies of SWCNT-based devices, although they are still in an embryonic stage, are comparable to those of devices with ITO electrodes [104,147,151].

Recently, conductive polymers have been tested for electromagnetic interference (EMI) shielding applications. A matrix containing SWCNTs is an attractive alternative for shielding [152,153], owing to its extremely low electrical percolation threshold. For 15% NT loading of a polymer composite, a 49 dB shielding effectiveness (SE) at 10 MHz has been reported by Li et al. [154]. Different SEs were achieved at the same SWCNT loading because of differences in conductivity. Longer CNTs lead to better SE. High frequency gave rise to larger skin depth, which then requires a larger thickness to achieve the same SE. Lim's group et al. [155] have measured the SE in the terahertz range using time-domain terahertz spectroscopy on thin layers of SWCNTs coated on flexible substrates, and the results are in good agreement with the Drude free-electron model. These films demonstrated good shielding of electromagnetic waves in the terahertz range, while transparency to visible light was maintained. They also found that the shielding efficiency can be engineered by thickness control of the SWCNT layer and/or by additional chemical treatment. For freestanding flexibly transparent nanocomposite films of continuous SWCNT bundle network and epoxy, Xie et al. [156] put forward an effective fabrication method and

characterized their SEs in the 10 MHz–20 GHz range. They found that a single layer of SWCNT bundle network was sufficient for substantial shielding and that the EMI shielding character of the nanocomposite was essentially determined by the layer of SWCNT bundle network, regardless of the polymer matrix. SEs at low frequency range (10 MHz–1.5 GHz) are more than 20 dB, which suggests that these nanocomposite films are promising as a type of ultralight, flexible, and transparent microwave shielding material.

5 Application as supercapacitors

Supercapacitors, also known as electrochemical capacitors, have attracted enormous interest because of their high power density (1–10 kW kg^{-1}), high energy density (0.5–10 Wh kg^{-1}), long cycle life (>10000 cycles), and light mass. Supercapacitors are considered to be one of the most promising energy conversion and storage devices to meet future energy storage needs [19,157–159], and are highlighted in a report from the US Department of Energy as being of equal importance with batteries [160]. According to the energy storage mechanism, supercapacitors can be classified into two categories, i.e., electrical double layer capacitors (EDLCs) and redox supercapacitors (pseudo-capacitors) [161]. CNTs, particularly SWCNTs, satisfy all the fundamental requirements for supercapacitor electrodes. The SWCNT bundle networks are ideal candidates for supercapacitors, because of their high accessible surface area of porous morphology, high electrical conductivity, low mass density, and chemical stability. There are several studies on the application of porous CNT electrodes for supercapacitors [147,162–170].

For EDLCs, the capacitance comes from the pure electrostatic charge accumulated at the electrode/electrolyte interface, which is strongly dependent on the surface area of the electrode materials accessible to the electrolyte ions. The large surface area of SWCNT networks is attributed to the high density of pores accessible to the mobile ions. Niu et al. [163] reported the first work on MWCNT-based supercapacitor electrodes in 1997. The fabricated supercapacitor showed specific capacitances of 102 F g^{-1} at 1 Hz and 49 F g^{-1} at 100 Hz, respectively, with surface area of 430 m^2 g^{-1} and a power density of 8 kW kg^{-1} in a 38% H_2SO_4 acidic electrolyte. This pioneering work stimulated increasing interest in CNTs as supercapacitor electrodes. Gruner et al. [171] employed SWCNT paper as EDLC electrodes and achieved a specific capacitance of 39 F g^{-1} and a power density of 5.8 kW kg^{-1} using 1 mol/L H_2SO_4 as the electrolyte.

Aligned CNTs were also used as supercapacitor electrodes. An ultralong (1.0 mm) aligned CNT array electrode achieved higher specific capacitance, lower equivalent series resistance, and better rate capability than the entangled CNT electrode, owing to the aligned CNT array electrode possessing larger pore size and more regular pore structure and conductive paths [172]. Futaba and co-workers [173] have presented a rational and general method to fabricate a very densely packed and aligned SWCNT material by using the zipping effect of liquids, which allowed the bulk materials to retain the intrinsic properties of the SWCNTs. They demonstrated the use of this dense SWCNT solid as supercapacitor electrodes, and could achieve an energy density of about 35 Wh kg^{-1} in an organic electrolyte. Previous studies of CNT electrodes have suffered from low surface area and chemical impurities hindering their performance. Recently, Izadi-Najafabadi et al. [168] made supercapacitor electrodes using solely the purest vertically aligned SWCNT arrays as starting materials. The energy density and power density of the SWCNT electrodes could reach 94 Wh kg^{-1} and 210 kW kg^{-1} respectively by operating at a higher voltage range of 4 V whilst maintaining durable full charge-discharge cyclability, which surpasses most other CNT electrodes reported. The combination of high surface area and electrochemical doping leads to a high specific capacitance of 160 F g^{-1}, further enhancing energy storage. These results reveal the full potential of SWCNTs as ideal supercapacitor electrodes.

For commercial applications, cycling up to 100000 cycles is generally required [161]. Recently, Wei et al. [174] assembled a supercapacitor with electrodes of SWCNT films, grown directly by CVD and purified without any filtration, and an organic electrolyte, and they revealed ultralong galvanostatic charge-discharge cycling over 200000 cycles in a coin cell structure at a current density of 20 A g^{-1} at 25 and 100°C, while maintaining 80% efficiency.

Thus far, CNT-based supercapacitors have not only manifested notable energy and power performance, but also enabled new functionalities such as stretchable [167], flexible [175], and transparent [147] supercapacitors. Since the area of SWCNT arrays is limited and difficult to scale up, most of the reported supercapacitors based on SWCNT array electrodes are in general of stacked design. The major challenge in realization of a rolled design for SWCNT film supercapacitors is the fabrication of large-area flexible conducting SWCNT film electrodes. Recently, Niu et al. [169] assembled compact-design supercapacitors using large-scaled freestanding and flexible SWCNT networks as both anode and cathode. A prototype of the processing procedures was developed to obtain uniform spreading of the SWCNT films onto the separators serving as both electrodes and charge collectors without metallic current collectors as shown in Figure 6, leading to a simplified and lightweight architecture. The area of SWCNT film on a separator can be scaled up and its thickness can be extended. High energy and power densities (43.7 Wh kg^{-1} and 197.3 kW kg^{-1}, respectively) were achieved for the prepared SWCNT film-based compact-design supercapacitors with small equivalent series resistance. The specific capacitance of this kind of compact-design SWCNT film supercapacitor is about

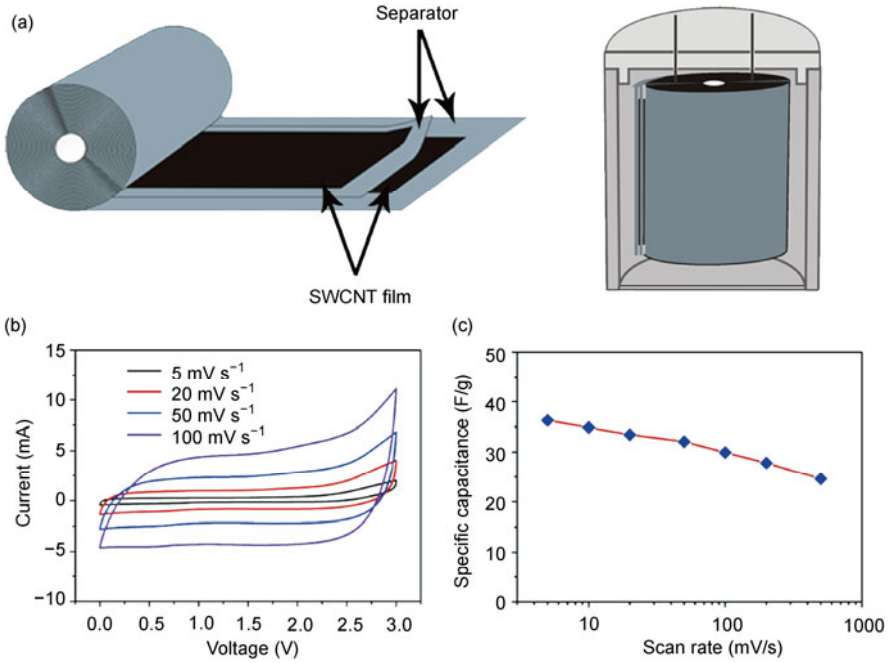

Figure 6 (a) Schematic diagram of assembling a compact-design supercapacitor using free-standing flexible SWCNT network: two pieces of separator coated with SWCNT films were stacked together and rolled up, then the compact-designed supercapacitor was assembled by filling with electrolyte. The performance of the compact-design supercapacitors using free-standing SWCNT films as both anode and cathode: (b) typical CVs at different scan rates; (c) the specific capacitance as a function of the scan rate. Reproduced with permission from ref. [169].

35 F g^{-1}. These results demonstrate that directly grown freestanding SWCNT films have significant potential as promising electrode materials for small, lightweight energy storage devices. Rolled design SWCNT film supercapacitors would bring in new opportunities for advanced applications in energy storage devices with high performance and lightweight architecture.

To fabricate transparent and flexible supercapacitors, Niu [83] put forward a novel strategy to prepare ultrathin SWCNT transparent and conductive films (TCFs) on a flexible and transparent substrate by combining direct-growth with transfer-printing methods. The as-prepared flexible and transparent SWCNT films on PET substrates were fabricated as a symmetrical two-electrode testing supercapacitor with good performance. First, an approach to processing freestanding SWCNT films was proposed to resolve their stickiness problem and to spread them out uniformly onto various substrates. This approach provides easy manipulation of the films, which will be beneficial for further applications of directly grown SWCNT films and may provide a technique for processing freestanding SWCNT films. Then, a "repeated transfer-printing" strategy is proposed to thin and separate a directly grown thick SWCNT film into many ultrathin SWCNT films. This transfer-printing technique, based on electrostatic adsorption, develops a transfer-printing technique and can be used to naturally transfer the SWCNT film from a substrate with high surface energy to another substrate with low surface energy. The "repeated transfer-printing" strategy effectively improves the utilization efficiency of SWCNTs and can better retain the uniformity of SWCNT films. Moreover, this method simplifies the experimental procedures or conditions and provides a simple, easy and highly efficient way of preparing ultrathin SWCNT TCFs.

The results presented above demonstrate that there is no pseudo-capacitance involved in the pure SWCNT network-based supercapacitors. For pseudo-capacitors, fast and reversible Faradic processes take place because of electroactive species. To develop high-capacitance supercapacitors, pseudo-capacitance must be introduced, by bringing foreign electroactive species into the porous carbon framework, in conjunction with the EDLC to enhance the overall capacitance of the electrode materials. The most commonly studied species that have quick and reversible Faradic reactions include oxygen- and nitrogen-containing surface functional groups, conductive polymers, and transition metal oxides (e.g., RuO_2, MnO_x). For example, supercapacitor electrodes prepared from a CNT/ruthenium oxide composite exhibited significantly higher specific capacitance because of a pseudocapacitance originating from the RuO_2 nanoparticles [176–178]. $Ni(OH)_2$/MWCNT composite positive electrodes and activated carbon negative electrodes delivered a specific energy of 32 Wh kg^{-1} at a specific power of 1500 W kg^{-1} based on the total weight of the active electrode materials [179]. A nickel oxide/CNT composite electrode resulted in an increased specific capacitance of 52 F g^{-1} [180]. An et al. [164] fabricated SWCNT/polypyrrole (PPy) nanocomposite electrodes and reported a much higher

specific capacitance than those of either pure PPy or SWCNTs electrodes, and they attributed the increase to the uniformly coated PPy on the SWCNTs. Frackowiak et al. [181] studied different modifications of CNT films. The capacitance increased from 50 F g^{-1} to 163 F g^{-1} after modification with 5 nm PPy. After KOH activation their capacitance values increased significantly from 15 F g^{-1} to ca. 100 F g^{-1} [182]. Tour et al. [183] obtained a 7-fold increase of capacitance using a pyrrole coating on a CNT surface. The power density and energy density showed dramatic improvement after the pyrrole coating on CNT films. The double layer capacitance for the bare CNT electrode was 10 F cm^{-2} and the pyrrole-modified CNT electrode was 145 F cm^{-2}. At 10 mA discharge current, the power density of pyrrole treated samples was almost 25 times that of the control "bucky paper". Zhou et al. [184] prepared SWCNT/polyaniline (PANI) composite electrodes by the polymerization of aniline containing well-dissolved SWCNTs and found much higher specific capacitances up to 190.6 F g^{-1}.

Recently, Niu [83] assembled flexible composite supercapacitors with large-scale freestanding SWCNT networks and PANI. The specific capacitance of this kind of supercapacitor was 236 F g^{-1}, while a value of 35 F g^{-1} was obtained for pure freestanding SWCNT networks. The specific capacitance was improved dramatically by the enhanced pseudo-capacitance because of the greater Faradic effect of the p-doping of PANI.

It is noted that most of the reported studies were done using a conventional energy-storage device configuration (a separator sandwiched between two electrodes sealed in liquid electrolyte), which prevents further reduction of the the device dimensions. A recent study by Meng et al. [185] demonstrated a novel kind of ultrathin all-solid-state supercapacitor configuration, prepared via an extremely simple process, using two slightly separated PANI-based electrodes well solidified in H_2SO_4-polyvinyl alcohol (PVA) gel electrolyte. The thickness of the entire device is comparable to that of a piece of standard A4 paper. Along with its highly flexible (twisting) state, the integrate device has a high specific capacitance of 350 F g^{-1} for the electrode materials, good cycle stability after 1000 cycles and a leakage current as small as 17.2 μA. Furthermore, owing to its polymer-based component structure, it has a specific capacitance as high as 31.4 F g^{-1} for the entire device, which is more than 6 times that of current high-level commercial supercapacitor products. These highly flexible, all-solid-state, paperlike polymer supercapacitors may bring new opportunities for designing configurations of energy-storage devices for future wearable electronics.

In spite of recent experimental and theoretical progress in supercapacitors based on SWCNT/MWCNT networks, there is still no comprehensive understanding of the charge storage mechanism in the nanoscale spaces, which hinders future investigation and developments. Therefore, the major challenges in this area at present include: (1) improving the surface area of CNT electrodes; (2) removal of chemical impurities, which might cause parasitic reactions that limit the lifetime and diminish capacitance; (3) optimizing the device parameters and the processing techniques for the electrodes and electrolytes to meet all relevant criteria for practical devices; (4) in-depth understanding of the mechanism regarding what happens during the microprocess or interfacial reactions and how the charge is stored inside the micropores; (5) exploring new nanocomposite electrodes or supercapacitors to overcome the present limitations and to push and widen their practical applications. Thus, more theoretical and fundamental studies on supercapacitors, based on the SWCNT networks and nanocomposite, are desired for their future development.

6 Conclusions and outlook

Thin films of SWCNTs represent an emerging class of materials [18,19], owing to their superior optical transparency, unique electric properties and mechanical flexibility, which come not only from the individual SWCNTs but also the collective behavior of the individual tubes with additional properties arising from the tube-tube interactions. Unlike isolated tubes, thin films of SWCNTs are suitable for scalable integration into devices to provide capabilities that are impossible or difficult to achieve with established inorganic materials. Much attention has been paid to their synthesis and characterization even as completely random networks. In this review, we have highlighted various aspects of a new kind of thin film — the "freestanding SWCNT bundle network", including its fabrication, fundamental properties, nanocomposites and application in supercapacitors.

2D SWCNT random networks can be easily prepared by either post-treatment, solution-based processes or direct CVD growth. Though the former can fabricate almost all SWCNT films with relatively low strength, the latter is most popular — in spite of its inconvenience for large-area substrates — as it is relatively easy to control the material's density, orientation, and so on, and organic contaminants that are undesirable in electronic devices can be avoided. Recently, freestanding SWCNT bundle networks with an area up to several tens of square centimeters and of various thicknesses, have been synthesized directly by a developed FCCVD technique [13,16]. Thereafter, several approaches have been used to fabricate this kind of freestanding network with controllable thickness up to sub-monolayer [83–86]. The freestanding SWCNT bundle networks exhibit superior optical transparency, unique electrical properties, good nonlinear optical properties and excellent mechanical flexibility as a result of their 2D reticulate architecture with extensive interbundle continuous connections like a "closed circuit". They are good candidates for use in thin film transistors, flexible electronics and chemical and biological

sensors; as optically transparent electrodes for use in solar cells and displays; as artificial actuators; as microwave shielding materials; as saturable absorbers used in mode-lock lasers or as ultrafast switching materials in optical telecommunications; as nano-scale reinforcement applied in nanocomposites; and as nanoporous electrodes for energy storage applications including batteries, fuel cells, and supercapacitors, and so forth [18,19]. Though a detailed understanding of how to control the overall optical and transport properties of transparent SWCNT networks has not yet emerged, and optimizing both properties simultaneously remains a problem, this lack of knowledge does not seem to inhibit some successful applications of the SWCNT thin films.

In addition, obvious degradation of mechanical properties of freestanding SWCNT bundle networks was observed, as compared to individual or bundles of SWCNTs, since only a small part of the macroscale strain comes from the axial extension of SWCNT bundles, as revealed by the changes of the G'-band in the *in situ* Raman scattering tests [124]. To develop SWCNT reinforced structures, new load-bearing and load-transfer structural units have been designed by improving the volume fraction and orientation of the tubes and by increasing the interface strength. Compared with "bucky paper" based high-SWCNT-content composites, the tensile strength of the new nanocomposites is more than one order of magnitude higher [140]. This result demonstrates that the true potential of CNTs, although it has not yet been fully realized in this new composite, can be achieved in nanocomposites, through load-transfer-favored three-dimensional architecture and molecular-level couplings with the polymer chains.

However, as reported in "The top ten advances in materials science" over the last 50 years [1], "today, the remarkable, unique, and phenomenally promising properties of these nanoscale carbon structures have placed them right among the hottest topics of materials science. So why are they only at number eight in this list? Well, there still remains much to sort out in their synthesis, purification, large-scale production, and assembly into devices. And there is also the very frustrating inability to manufacture uniform samples of nanotubes with the same properties." These prominent obstacles severely hamper further development in this field. In addition to these common problems, for macro-scale SWCNT networks, some special issues, such as scale-up of current processes to produce continuous network, and the efficiency of transferring the properties of SWCNTs to the micro- and macro-structural levels, still require much attention. For SWCNT reinforced nanocomposite films/fibers, some significant challenges are obviously to elucidate the interfacial structure and interfacial coupling strength, and to transfer and retain the unique properties of individual SWCNTs. Overcoming these obstacles is a prerequisite for SWCNTs to bring about a revolution in materials science.

This work was supported by the National Natural Science Foundation of China (10334060, 50572119, 90921012, 51172271), the National Basic Research Program of China (2005CB623602, 2012CB932302), Beijing Municipal Education Commission (YB20108000101) and the Key Item of Knowledge Innovation Project of Chinese Academy of Sciences (KJCX2-YW-M01).

1 Wood J. The top ten advances in materials science. Mater Today, 2008, 11: 40–45
2 Hamada N, Sawada S, Oshiyama A. New one-dimensional conductors — Graphitic microtubules. Phys Rev Lett, 1992, 68: 1579–1581
3 White C T, Todorov T N. Carbon nanotubes as long ballistic conductors. Nature, 1998, 393: 240–242
4 Yao Z, Kane C L, Dekker C. High-field electrical transport in single-wall carbon nanotubes. Phys Rev Lett, 2000, 84: 2941–2944
5 Dai H J, Pop E, Mann D, et al. Thermal conductance of an individual single-wall carbon nanotube above room temperature. Nano Lett, 2006, 6: 96–100
6 Salvetat J P, Briggs G A D, Bonard J M, et al. Elastic and shear moduli of single-walled carbon nanotube ropes. Phys Rev Lett, 1999, 82: 944–947
7 Wong E W, Sheehan P E, Lieber C M. Nanobeam mechanics: Elasticity, strength, and toughness of nanorods and nanotubes. Science, 1997, 277: 1971–1975
8 Yu M F, Files B S, Arepalli S, et al. Tensile loading of ropes of single wall carbon nanotubes and their mechanical properties. Phys Rev Lett, 2000, 84: 5552–5555
9 Khang D Y, Xiao J L, Kocabas C, et al. Molecular scale buckling mechanics on individual aligned single-wall carbon nanotubes on elastomeric substrates. Nano Lett, 2008, 8: 124–130
10 Treacy M M J, Ebbesen T W, Gibson J M. Exceptionally high Young's modulus observed for individual carbon nanotubes. Nature, 1996, 381: 678–680
11 Pan Z W, Xie S S, Lu L, et al. Tensile tests of ropes of very long aligned multiwall carbon nanotubes. Appl Phys Lett, 1999, 74: 3152–3154
12 Walters D A, Ericson L M, Casavant M J, et al. Elastic strain of freely suspended single-wall carbon nanotube ropes. Appl Phys Lett, 1999, 74: 3803–3805
13 Song L, Ci L, Lv L, et al. Direct synthesis of a macroscale single-walled carbon nanotube non-woven material. Adv Mater, 2004, 16: 1529–1534
14 Zhao X L, Inoue S, Jinno M, et al. Macroscopic oriented web of single-wall carbon nanotubes. Chem Phys Lett, 2003, 373: 266–271
15 Liu Q F, Fujigaya T, Cheng H M, et al. Free-standing highly conductive transparent ultrathin single-walled carbon nanotube films. J Am Chem Soc, 2010, 132: 16581–16586
16 Ma W J, Song L, Yang R, et al. Directly synthesized strong, highly conducting, transparent single-walled carbon nanotube films. Nano Lett, 2007, 7: 2307–2311
17 Skakalova V, Kaiser A B, Woo Y S, et al. Electronic transport in carbon nanotubes: From individual nanotubes to thin and thick networks. Phys Rev B, 2006, 74: 085403
18 Cao Q, Rogers J A. Ultrathin films of single-walled carbon nanotubes for electronics and sensors: A review of fundamental and applied aspects. Adv Mater, 2009, 21: 29–53
19 Hu L B, Hecht D S, Gruner G. Carbon nanotube thin films: Fabrication, properties, and applications. Chem Rev, 2010, 110: 5790–5844
20 Hecht D S, Hu L B, Irvin G. Emerging transparent electrodes based on thin films of carbon nanotubes, graphene, and metallic nanostructures. Adv Mater, 2011, 23: 1482–1513
21 Zhou W Y, Bai X D, Wang E G, et al. Synthesis, structure, and properties of single-walled carbon nanotubes. Adv Mater, 2009, 21: 4565–4583
22 Schnorr J M, Swager T M. Emerging applications of carbon nanotubes. Chem Mater, 2011, 23: 646–657

23 Rinzler A G, Liu J, Dai H, et al. Large-scale purification of single-wall carbon nanotubes: Process, product, and characterization. Appl Phys A: Mater Sci Process, 1998, 67: 29–37
24 Sreekumar T V, Liu T, Kumar S, et al. Single-wall carbon nanotube films. Chem Mater, 2003, 15: 175–178
25 Hu L B, Hecht D S, Gruner G. Percolation in transparent and conducting carbon nanotube networks. Nano Lett, 2004, 4: 2513–2517
26 Burghard M, Duesberg G, Philipp G, et al. Controlled adsorption of carbon nanotubes on chemically modified electrode arrays. Adv Mater, 1998, 10: 584–588
27 Lay M D, Novak J P, Snow E S. Simple route to large-scale ordered arrays of liquid-deposited carbon nanotubes. Nano Lett, 2004, 4: 603–606
28 Rao S G, Huang L, Setyawan W, et al. Large-scale assembly of carbon nanotubes. Nature, 2003, 425: 36–37
29 Shimoda H, Oh S J, Geng H Z, et al. Self-assembly of carbon nanotubes. Adv Mater, 2002, 14: 899–901
30 Tulevski G S, Hannon J, Afzali A, et al. Chemically assisted directed assembly of carbon nanotubes for the fabrication of large-scale device arrays. J Am Chem Soc, 2007, 129: 11964–11968
31 Lee M, Im J, Lee B Y, et al. Linker-free directed assembly of high-performance integrated devices based on nanotubes and nanowires. Nat Nanotechnol, 2006, 1: 66–71
32 Krstic V, Duesberg G S, Muster J, et al. Langmuir-Blodgett films of matrix-diluted single-walled carbon nanotubes. Chem Mater, 1998, 10: 2338–2340
33 Guo Y Z, Minami N, Kazaoui S, et al. Multi-layer LB films of single-wall carbon nanotubes. Physica B, 2002, 323: 235–236
34 Li X L, Zhang L, Wang X R, et al. Langmuir-Blodgett assembly of densely aligned single-walled carbon nanotubes from bulk materials. J Am Chem Soc, 2007, 129: 4890–4891
35 Saran N, Parikh K, Suh D S, et al. Fabrication and characterization of thin films of single-walled carbon nanotube bundles on flexible plastic substrates. J Am Chem Soc, 2004, 126: 4462–4463
36 Jang E Y, Kang T J, Im H, et al. Macroscopic single-walled-carbon-nanotube fiber self-assembled by dip-coating method. Adv Mater, 2009, 21: 4357–4361
37 Kaempgen M, Duesberg G S, Roth S. Transparent carbon nanotube coatings. Appl Surf Sci, 2005, 252: 425–429
38 Kim S, Yim J, Wang X, et al. Spin- and spray-deposited single-walled carbon-nanotube electrodes for organic solar cells. Adv Funct Mater, 2010, 20: 2310–2316
39 Zhou Y X, Gaur A, Hur S H, et al. p-channel, n-channel thin film transistors and p-n diodes based on single wall carbon nanotube networks. Nano Lett, 2004, 4: 2031–2035
40 LeMieux M C, Roberts M, Barman S, et al. Self-sorted, aligned nanotube networks for thin-film transistors. Science, 2008, 321: 101–104
41 Meitl M A, Zhou Y X, Gaur A, et al. Solution casting and transfer printing single-walled carbon nanotube films. Nano Lett, 2004, 4: 1643–1647
42 Endo M, Muramatsu H, Hayashi T, et al. 'Buckypaper' from coaxial nanotubes. Nature, 2005, 433: 476
43 Hall L J, Coluci V R, Galvao D S, et al. Sign change of Poisson's ratio for carbon nanotube sheets. Science, 2008, 320: 504–507
44 Chew S Y, Ng S H, Wang J, et al. Flexible free-standing carbon nanotube films for model lithium-ion batteries. Carbon, 2009, 47: 2976–2983
45 Beecher P, Servati P, Rozhin A, et al. Ink-jet printing of carbon nanotube thin film transistors. J Appl Phys, 2007, 102: 043710
46 Park J U, Hardy M, Kang S J, et al. High-resolution electro-hydrodynamic jet printing. Nat Mater, 2007, 6: 782–789
47 Kordas K, Mustonen T, Toth G, et al. Inkjet printing of electrically conductive patterns of carbon nanotubes. Small, 2006, 2: 1021–1025
48 Jiang K, Wang J, Li Q, et al. Superaligned carbon nanotube arrays, films, and yarns: A road to applications. Adv Mater, 2011, 23: 1154–1161
49 Zhang M, Fang S L, Zakhidov A A, et al. Strong, transparent, multifunctional, carbon nanotube sheets. Science, 2005, 309: 1215–1219
50 Dai H J, Rinzler A G, Nikolaev P, et al. Single-wall nanotubes produced by metal-catalyzed disproportionation of carbon monoxide. Chem Phys Lett, 1996, 260: 471–475
51 Hafner J H, Bronikowski M J, Azamian B R, et al. Catalytic growth of single-wall carbon nanotubes from metal particles. Chem Phys Lett, 1998, 296: 195–202
52 Nikolaev P, Bronikowski M J, Bradley R K, et al. Gas-phase catalytic growth of single-walled carbon nanotubes from carbon monoxide. Chem Phys Lett, 1999, 313: 91–97
53 Fonseca A, Hernadi K, Piedigrosso P, et al. Synthesis of single- and multi-wall carbon nanotubes over supported catalysts. Appl Phys A: Mater Sci Process, 1998, 67: 11–22
54 Franklin N R, Dai H J. An enhanced CVD approach to extensive nanotube networks with directionality. Adv Mater, 2000, 12: 890–894
55 Li Y L, Zhang L H, Zhong X H, et al. Synthesis of high purity single-walled carbon nanotubes from ethanol by catalytic gas flow CVD reactions. Nanotechnol, 2007, 18: 225604
56 Maruyama S, Kojima R, Miyauchi Y, et al. Low-temperature synthesis of high-purity single-walled carbon nanotubes from alcohol. Chem Phys Lett, 2002, 360: 229–234
57 Cassell A M, Raymakers J A, Kong J, et al. Large scale CVD synthesis of single-walled carbon nanotubes. J Phys Chem B, 1999, 103: 6484–6492
58 Su M, Zheng B, Liu J. A scalable CVD method for the synthesis of single-walled carbon nanotubes with high catalyst productivity. Chem Phys Lett, 2000, 322: 321–326
59 Cheng H M, Li F, Su G, et al. Large-scale and low-cost synthesis of single-walled carbon nanotubes by the catalytic pyrolysis of hydrocarbons. Appl Phys Lett, 1998, 72: 3282–3284
60 Cheng H M, Li F, Sun X, et al. Bulk morphology and diameter distribution of single-walled carbon nanotubes synthesized by catalytic decomposition of hydrocarbons. Chem Phys Lett, 1998, 289: 602–610
61 Satishkumar B C, Govindaraj A, Sen R, et al. Single-walled nanotubes by the pyrolysis of acetylene-organometallic mixtures. Chem Phys Lett, 1998, 293: 47–52
62 Bronikowski M J, Willis P A, Colbert D T, et al. Gas-phase production of carbon single-walled nanotubes from carbon monoxide via the HiP_{CO} process: A parametric study. J Vac Sci Technol, A, 2001, 19: 1800–1805
63 Wei B Q, Vajtai R, Jung Y, et al. Organized assembly of carbon nanotubes—Cunning refinements help to customize the architecture of nanotube structures. Nature, 2002, 416: 495–496
64 Kong J, Cassell A M, Dai H J. Chemical vapor deposition of methane for single-walled carbon nanotubes. Chem Phys Lett, 1998, 292: 567–574
65 Yan Y H, Chan-Park M B, Zhang Q. Advances in carbon-nanotube assembly. Small, 2007, 3: 24–42
66 Huang S M, Cai X Y, Du C S, et al. Oriented long single walled carbon nanotubes on substrates from floating catalysts. J Phys Chem B, 2003, 107: 13251–13254
67 Zhang Y G, Chang A L, Cao J, et al. Electric-field-directed growth of aligned single-walled carbon nanotubes. Appl Phys Lett, 2001, 79: 3155–3157
68 Ural A, Li Y M, Dai H J. Electric-field-aligned growth of single-walled carbon nanotubes on surfaces. Appl Phys Lett, 2002, 81: 3464–3466
69 Joselevich E, Lieber C M. Vectorial growth of metallic and semiconducting single-wall carbon nanotubes. Nano Lett, 2002, 2: 1137–1141
70 Xie S S, Song L, Ci L J, et al. Controllable preparation and properties of single-/double-walled carbon nanotubes. Sci Technol Adv Mater, 2005, 6: 725–735
71 Hata K, Futaba D N, Mizuno K, et al. Water-assisted highly efficient synthesis of impurity-free single-waited carbon nanotubes. Science, 2004, 306: 1362–1364

72 Amama P B, Pint C L, McJilton L, et al. Role of water in super growth of single-walled carbon nanotube carpets. Nano Lett, 2009, 9: 44–49
73 Kang S J, Kocabas C, Ozel T, et al. High-performance electronics using dense, perfectly aligned arrays of single-walled carbon nanotubes. Nat Nanotechnol, 2007, 2: 230–236
74 Kocabas C, Hur S H, Gaur A, et al. Guided growth of large-scale, horizontally aligned arrays of single-walled carbon nanotubes and their use in thin-film transistors. Small, 2005, 1: 1110–1116
75 Kocabas C, Kang S J, Ozel T, et al. Improved synthesis of aligned arrays of single-walled carbon nanotubes and their implementation in thin film type transistors. J Phys Chem C, 2007, 111: 17879–17886
76 Ding L, Tselev A, Wang J Y, et al. Selective growth of well-aligned semiconducting single-walled carbon nanotubes. Nano Lett, 2009, 9: 800–805
77 Pint C L, Xu Y Q, Pasquali M, et al. Formation of highly dense aligned ribbons and transparent films of single-walled carbon nanotubes directly from carpets. ACS Nano, 2008, 2: 1871–1878
78 Zhou Z P, Ci L J, Song L, et al. Random networks of single-walled carbon nanotubes. J Phys Chem B, 2004, 108: 10751–10753
79 Zhou Z P, Wan D Y, Dou X Y, et al. Surface-enhanced Raman scattering from the individual metallic single-walled carbon nanotubes. Physica E, 2005, 28: 360–364
80 Zhou Z P, Ci L, Song L, et al. The intrinsic temperature effect of Raman spectra of double-walled carbon nanotubes. Chem Phys Lett, 2004, 396: 372–376
81 Ci L J, Zhou Z P, Tang D S, et al. Double wall carbon nanotubes with an inner diameter of 0.4 nm. Chem Vap Deposition, 2003, 9: 119–121
82 Zhou Z P, Wan D Y, Dou X Y, et al. Postgrowth alignment of SWNTs by an electric field. Carbon, 2006, 44: 170–173
83 Niu Z Q. Studies on the preparation and properties of carbon nanotube films and electrochemical devices. Doctor Dissertation. Beijing: Graduate School of the Chinese Academy of Sciences, 2010
84 Nasibulin A G, Kaskela A, Mustonen K, et al. Multifunctional free-standing single-walled carbon nanotube films. ACS Nano, 2011, 5: 3214–3221
85 Wang H F, Ghosh K, Li Z H, et al. Direct growth of single-walled carbon nanotube films and their optoelectric properties. J Phys Chem C, 2009, 113: 12079–12084
86 Fraser I S, Motta M S, Schmidt R K, et al. Continuous production of flexible carbon nanotube-based transparent conductive films. Sci Technol Adv Mater, 2010, 11: 045004
87 Smith B W, Benes Z, Luzzi D E, et al. Structural anisotropy of magnetically aligned single wall carbon nanotube films. Appl Phys Lett, 2000, 77: 663–665
88 Kim W, Choi H C, Shim M, et al. Synthesis of ultralong and high percentage of semiconducting single-walled carbon nanotubes. Nano Lett, 2002, 2: 703–708
89 Fischer J E, Dai H, Thess A, et al. Metallic resistivity in crystalline ropes of single-wall carbon nanotubes. Phys Rev B, 1997, 55: R4921–R4924
90 Wu Z C, Chen Z H, Du X, et al. Transparent, conductive carbon nanotube films. Science, 2004, 305: 1273–1276
91 Bekyarova E, Itkis M E, Cabrera N, et al. Electronic properties of single-walled carbon nanotube networks. J Am Chem Soc, 2005, 127: 5990–5995
92 Skakalova V, Kaiser A B, Dettlaff-Weglikowska U, et al. Effect of chemical treatment on electrical conductivity, infrared absorption, and Raman spectra of single-walled carbon nanotubes. J Phys Chem B, 2005, 109: 7174–7181
93 Kocabas C, Pimparkar N, Yesilyurt O, et al. Experimental and theoretical studies of transport through large scale, partially aligned arrays of single-walled carbon nanotubes in thin film type transistors. Nano Lett, 2007, 7: 1195–1202
94 Yang Y, Wang L, Yan H, et al. Highly transparent and conductive double-layer oxide thin films as anodes for organic light-emitting diodes. Appl Phys Lett, 2006, 89: 051116
95 Hone J, Llaguno M C, Nemes N M, et al. Electrical and thermal transport properties of magnetically aligned single walt carbon nanotube films. Appl Phys Lett, 2000, 77: 666–668
96 Durkop T, Getty S A, Cobas E, et al. Extraordinary mobility in semiconducting carbon nanotubes. Nano Lett, 2004, 4: 35–39
97 Thostenson E T, Ren Z F, Chou T W. Advances in the science and technology of carbon nanotubes and their composites: A review. Compos Sci Technol, 2001, 61: 1899–1912
98 Artukovic E, Kaempgen M, Hecht D, et al. Transparent and flexible carbon nanotube transistors. Nano Lett, 2005, 5: 757–760
99 Takenobu T, Takahashi T, Kanbara T, et al. High-performance transparent flexible transistors using carbon nanotube films. Appl Phys Lett, 2006, 88: 033511
100 Cao Q, Hur S H, Zhu Z T, et al. Highly bendable, transparent thin-film transistors that use carbon-nanotube-based conductors and semiconductors with elastomeric dielectrics. Adv Mater, 2006, 18: 304–309
101 Javey A, Guo J, Wang Q, et al. Ballistic carbon nanotube field-effect transistors. Nature, 2003, 424: 654–657
102 Kong J, Yenilmez E, Tombler T W, et al. Quantum interference and ballistic transmission in nanotube electron waveguides. Phys Rev Lett, 2001, 87: 106801
103 Pasquier A D, Unalan H E, Kanwal A, et al. Conducting and transparent single-wall carbon nanotube electrodes for polymer-fullerene solar cells. Appl Phys Lett, 2005, 87: 203511
104 Ishikawa F N, Chang H K, Ryu K, et al. Transparent electronics based on transfer printed aligned carbon nanotubes on rigid and flexible substrates. ACS Nano, 2009, 3: 73–79
105 Blackburn J L, Barnes T M, Beard M C, et al. Transparent conductive single-walled carbon nanotube networks with precisely tunable ratios of semiconducting and metallic nanotubes. ACS Nano, 2008, 2: 1266–1274
106 Dresselhaus M S, Eklund P C. Phonons in carbon nanotubes. Adv Phys, 2000, 49: 705–814
107 Xie R H, Jiang J. Nonlinear optical properties of armchair nanotube. Appl Phys Lett, 1997, 71: 1029–1031
108 Liu X C, Si J H, Chang B H, et al. Third-order optical nonlinearity of the carbon nanotubes. Appl Phys Lett, 1999, 74: 164–166
109 Lauret J S, Voisin C, Cassabois G, et al. Ultrafast carrier dynamics in single-wall carbon nanotubes. Phys Rev Lett, 2003, 90: 57404
110 Nemilentsau A M, Slepyan G Y, Khrutchinskii A A, et al. Third-order optical nonlinearity in single-wall carbon nanotubes. Carbon, 2006, 44: 2246–2253
111 Xie S S, Li W Z, Pan Z W, et al. Mechanical and physical properties on carbon nanotube. J Phys Chem Solids, 2000, 61: 1153–1158
112 Chen Y C, Raravikar N R, Schadler L S, et al. Ultrafast optical switching properties of single-wall carbon nanotube polymer composites at 1.55 μm. Appl Phys Lett, 2002, 81: 975–977
113 Maeda A, Matsumoto S, Kishida H, et al. Large optical nonlinearity of semiconducting single-walled carbon nanotubes under resonant excitations. Phys Rev Lett, 2005, 94: 47404
114 Tatsuura S, Furuki M, Sato Y, et al. Semiconductor carbon nanotubes as ultrafast switching materials for optical telecommunications. Adv Mater, 2003, 15: 534–537
115 Long Y B, Song L, Li C Y, et al. Revealing two-competing processes in carrier dynamics of single-walled carbon nanotube films. Chem Phys Lett, 2005, 405: 300–303
116 Ma W J, Feng B H, Ren Y, et al. Large third-order optical nonlinearity in directly synthesized single-walled carbon nanotube films. J Nanosci Nanotechnol, 2010, 10: 7333–7335
117 Wang F, Rozhin A G, Scardaci V, et al. Wideband-tuneable, nanotube mode-locked, fibre laser. Nat Nanotechnol, 2008, 3: 738–742
118 Yu M F, Lourie O, Dyer M J, et al. Strength and breaking mechanism of multiwalled carbon nanotubes under tensile load. Science, 2000, 287: 637–640
119 Kataura H, Kumazawa Y, Maniwa Y, et al. Optical properties of single-wall carbon nanotubes. Synth Met, 1999, 103: 2555–2558
120 Baughman R H, Zakhidov A A, de Heer W A. Carbon nanotubes —

The route toward applications. Science, 2002, 297: 787–792
121 Ajayan P M, Schadler L S, Giannaris C, et al. Single-walled carbon nanotube-polymer composites: Strength and weakness. Adv Mater, 2000, 12: 750–753
122 Kis A, Csanyi G, Salvetat J P, et al. Reinforcement of single-walled carbon nanotube bundles by intertube bridging. Nat Mater, 2004, 3: 153–157
123 Qian D, Liu W K, Ruoff R S. Load transfer mechanism in carbon nanotube ropes. Compos Sci Technol, 2003, 63: 1561–1569
124 Ma W J, Liu L Q, Yang R, et al. Monitoring a micromechanical process in macroscale carbon nanotube films and fibers. Adv Mater, 2009, 21: 603–608
125 Zhang X F, Sreekumar T V, Liu T, et al. Properties and structure of nitric acid oxidized single wall carbon nanotube films. J Phys Chem B, 2004, 108: 16435–16440
126 Koziol K, Vilatela J, Moisala A, et al. High-performance carbon nanotube fiber. Science, 2007, 318: 1892–1895
127 Cronin S B, Swan A K, Unlu M S, et al. Resonant Raman spectroscopy of individual metallic and semiconducting single-wall carbon nanotubes under uniaxial strain. Phys Rev B, 2005, 72: 035425
128 Zhang M, Atkinson K R, Baughman R H. Multifunctional carbon nanotube yarns by downsizing an ancient technology. Science, 2004, 306: 1358–1361
129 Jiang K L, Li Q Q, Fan S S. Nanotechnology: Spinning continuous carbon nanotube yarns — Carbon nanotubes weave their way into a range of imaginative macroscopic applications. Nature, 2002, 419: 801
130 Zhang X F, Li Q W, Holesinger T G, et al. Ultrastrong, stiff, and lightweight carbon-nanotube fibers. Adv Mater, 2007, 19: 4198–4201
131 Adams W W, Green M J, Behabtu N, et al. Nanotubes as polymers. Polymer, 2009, 50: 4979–4997
132 Yakobson B I, Campbell M P, Brabec C J, et al. High strain rate fracture and C-chain unraveling in carbon nanotubes. Comput Mater Sci, 1997, 8: 341–348
133 Liu L Q, Ma W J, Zhang Z. Macroscopic carbon nanotube assemblies: Preparation, properties, and potential applications. Small, 2011, 7: 1504–1520
134 Chou T W, Thostenson E T, Li C Y. Nanocomposites in context. Compos Sci Technol, 2005, 65: 491–516
135 Coleman J N, Khan U, Gun'ko Y K. Mechanical reinforcement of polymers using carbon nanotubes. Adv Mater, 2006, 18: 689–706
136 Gao Y, Li L Y, Tan P H, et al. Application of Raman spectroscopy in carbon nanotube-based polymer composites. Chin Sci Bull, 2010, 55: 3978–3988
137 Fisher F T, Bradshaw R D, Brinson L C. Fiber waviness in nanotube-reinforced polymer composites-1: Modulus predictions using effective nanotube properties. Compos Sci Technol, 2003, 63: 1689–1703
138 Ajayan P M, Tour J M. Materials science—Nanotube composites. Nature, 2007, 447: 1066–1068
139 Pan Z W, Xie S S, Chang B H, et al. Very long carbon nanotubes. Nature, 1998, 394: 631–632
140 Ma W J, Liu L Q, Zhang Z, et al. High-strength composite fibers: Realizing true potential of carbon nanotubes in polymer matrix through continuous reticulate architecture and molecular level couplings. Nano Lett, 2009, 9: 2855–2861
141 Chou T W, Gao L M, Thostenson E T, et al. An assessment of the science and technology of carbon nanotube-based fibers and composites. Compos Sci Technol, 2010, 70: 1–19
142 Tibbetts G G, Lake M L, Strong K L, et al. A review of the fabrication and properties of vapor-grown carbon nanofiber/polymer composites. Compos Sci Technol, 2007, 67: 1709–1718
143 Li C, Chou T W. Precise Determination of backbone structure and conductivity of 3d percolation networks by the direct electrifying algorithm. Inter J Mod Phys C, 2009, 20: 423–433
144 Li C, Thostenson E T, Chou T W. Effect of nanotube waviness on the electrical conductivity of carbon nanotube-based composites. Compos Sci Technol, 2008, 68: 1445–1452
145 Song L, Zhang H, Zhang Z, et al. Processing and performance improvements of SWNT paper reinforced PEEK nanocomposites. Compos Part A, 2007, 38: 388–392
146 Gruner G. Carbon nanotube films for transparent and plastic electronics. J Mater Chem, 2006, 16: 3533–3539
147 Chen P C, Shen G, Sukcharoenchoke S, et al. Flexible and transparent supercapacitor based on In_2O_3 nanowire/carbon nanotube heterogeneous films. Appl Phys Lett, 2009, 94: 043113
148 Shan B, Cho K J. First principles study of work functions of single wall carbon nanotubes. Phys Rev Lett, 2005, 94: 236602
149 Zhang D H, Ryu K, Liu X L, et al. Transparent, conductive, and flexible carbon nanotube films and their application in organic light-emitting diodes. Nano Lett, 2006, 6: 1880–1886
150 Rowell M W, Topinka M A, McGehee M D, et al. Organic solar cells with carbon nanotube network electrodes. Appl Phys Lett, 2006, 88: 233506
151 Liu Z, Zheng K H, Hu L J, et al. Surface-energy generator of single-walled carbon nanotubes and usage in a self-powered system. Adv Mater, 2010, 22: 999–1003
152 Lee B O, Woo W J, Kim M S. EMI shielding effectiveness of carbon nanofiber filled poly(vinyl alcohol) coating materials. Macromol Mater Eng, 2001, 286: 114–118
153 Das N C, Khastgir D, Chaki T K, et al. Electromagnetic interference shielding effectiveness of carbon black and carbon fibre filled EVA and NR based composites. Compos Part A, 2000, 31: 1069–1081
154 Li N, Huang Y, Du F, et al. Electromagnetic interference (EMI) shielding of single-walled carbon nanotube epoxy composites. Nano Lett, 2006, 6: 1141–1145
155 Seo M A, Yim J H, Ahn Y H, et al. Terahertz electromagnetic interference shielding using single-walled carbon nanotube flexible films. Appl Phys Lett, 2008, 93: 231905
156 Yi X S, Xie S S, Liu G, et al. Fabrication method of composites developed by carbon nanotube non-woven films for electromagnetic interference shielding. China Patent, ZL 200710195105.7, 2009-09-09
157 Simon P, Gogotsi Y. Materials for electrochemical capacitors. Nat Mater, 2008, 7: 845–854
158 Zhao X S, Zhang L L. Carbon-based materials as supercapacitor electrodes. Chem Soc Rev, 2009, 38: 2520–2531
159 Cheng H M, Liu C, Li F, et al. Advanced materials for energy storage. Adv Mater, 2010, 22: E28–E62
160 US Department of Energy, Basic research needs for electrical energy storage 2007. http://www.sc.doe.gov/bes/reports/abstracts.html, 2010
161 Conway B E. Electrochemical Supercapacitors: Scientific Fundamentals and Technological Applications. New York: Springer, 1999
162 Lee Y H, An K H, Kim W S, et al. Electrochemical properties of high-power supercapacitors using single-walled carbon nanotube electrodes. Adv Funct Mater, 2001, 11: 387–392
163 Niu C M, Sichel E K, Hoch R, et al. High power electrochemical capacitors based on carbon nanotube electrodes. Appl Phys Lett, 1997, 70: 1480–1482
164 An K H, Jeon K K, Heo J K, et al. High-capacitance supercapacitor using a nanocomposite electrode of single-walled carbon nanotube and polypyrrole. J Electrochem Soc, 2002, 149: A1058–A1062
165 Gupta V, Miura N. Polyaniline/single-wall carbon nanotube (PANI/SWCNT) composites for high performance supercapacitors. Electrochim Acta, 2006, 52: 1721–1726
166 Cui Y, Kaempgen M, Chan C K, et al. Printable thin film supercapacitors using single-walled carbon nanotubes. Nano Lett, 2009, 9: 1872–1876
167 Cui Y, Hu L B, Pasta M, et al. Stretchable, porous, and conductive energy textiles. Nano Lett, 2010, 10: 708–714
168 Izadi-Najafabadi A, Yasuda S, Kobashi K, et al. Extracting the full potential of single-walled carbon nanotubes as durable supercapacitor electrodes operable at 4 V with high power and energy density. Adv Mater, 2010, 22: E235–E241
169 Niu Z Q, Zhou W Y, Chen J, et al. Compact-designed supercapacitors using free-standing single-walled carbon nanotube films. Energy Environ Sci, 2011, 4: 1440–1446
170 Wang T, Kiebele A, Ma J, et al. Charge transfer between polyaniline

and carbon nanotubes supercapacitors: Improving both energy and power densities. J Electrochem Soc, 2011, 158: A1–A5
171 Gruner G, Kaempgen M, Ma J, et al. Bifunctional carbon nanotube networks for supercapacitors. Appl Phys Lett, 2007, 90: 264104
172 Zhang H, Cao G P, Yang Y S, et al. Comparison between electrochemical properties of aligned carbon nanotube array and entangled carbon nanotube electrodes. J Electrochem Soc, 2008, 155: K19–K22
173 Hata K, Futaba D N, Yamada T, et al. Shape-engineerable and highly densely packed single-walled carbon nanotubes and their application as super-capacitor electrodes. Nat Mater, 2006, 5: 987–994
174 Wei B Q, Masarapu C, Zeng H F, et al. Effect of temperature on the capacitance of carbon nanotube supercapacitors. ACS Nano, 2009, 3: 2199–2206
175 Pushparaj V L, Shaijumon M M, Kumar A, et al. Flexible energy storage devices based on nanocomposite paper. Proc Natl Acad Sci USA, 2007, 104: 13574–13577
176 Wang X F, Wang D Z, Liang L, et al. Electrochemical performance of RuO_2/active carbon, composite electrodes. Acta Phys: Chim Sin, 2002, 18: 750–753
177 Kim Y T, Tadai K, Mitani T. Highly dispersed ruthenium oxide nanoparticles on carboxylated carbon nanotubes for supercapacitor electrode materials. J Mater Chem, 2005, 15: 4914–4921
178 Joo O S, Lee J K, Pathan H M, et al. Electrochemical capacitance of nanocomposite films formed by loading carbon nanotubes with ruthenium oxide. J Power Sources, 2006, 159: 1527–1531
179 Wang Y G, Yu L, Xia Y Y. Electrochemical capacitance performance of hybrid supercapacitors based on $Ni(OH)_2$/carbon nanotube composites and activated carbon. J Electrochem Soc, 2006, 153: A743–A748
180 Wang X F, Wang D Z, Liang L. Electrochemical capacitor using nickel oxide/carbon nanotube composites electrode. J Inorg Mater, 2003, 18: 331–336
181 Frackowiak E, Jurewicz K, Szostak K, et al. Nanotubular materials as electrodes for supercapacitors. Fuel Process Technol, 2002, 77: 213–219
182 Frackowiak E, Jurewicz K, Beguin F. Development of new supercapacitor electrodes based on carbon nanotubes. Pol J Chem, 2004, 78: 1345–1356
183 Kumar S, Zhou C F, Doyle C D, et al. Functionalized single wall carbon nanotubes treated with pyrrole for electrochemical supercapacitor membranes. Chem Mater, 2005, 17: 1997–2002
184 Li H I, Zhou Y K, He B L, et al. Electrochemical capacitance of well-coated single-walled carbon nanotube with polyaniline composites. Electrochim Acta, 2004, 49: 257–262
185 Meng C, Liu C, Chen L, et al. Highly flexible and all-solid-state paperlike polymer supercapacitors. Nano Lett, 2010, 10: 4025–4031